

## **Glial Ca<sup>2+</sup> Signaling Controls Endocytosis and K<sup>+</sup> Buffering to Regulate Glial-Neuronal Communication at the Soma**

Shirley Weiss, Jan E. Melom, Kiel G. Ormerod, Yao V. Zhang and J. Troy Littleton

The Picower Institute for Learning and Memory

Department of Biology and Department of Brain and Cognitive Sciences

Massachusetts Institute of Technology

Cambridge, Massachusetts 02139

Correspondence and requests for materials should be addressed to S.W. ([s\\_weiss@mit.edu](mailto:s_weiss@mit.edu))

## **Summary**

Glial-neuronal signaling at synapses is widely appreciated, but how glia interact with neuronal cell bodies is less clear. *Drosophila* cortex glia are restricted to brain regions devoid of synapses, providing an opportunity to characterize interactions between glia and neuronal somas. Mutations in the cortex glial NCKX exchanger *zydeco* abolish microdomain  $\text{Ca}^{2+}$  oscillatory activity and elevate glial  $\text{Ca}^{2+}$ , predisposing animals to seizures. To determine how cortex glial  $\text{Ca}^{2+}$  signaling controls neuronal excitability, an *in vivo* modifier screen for the *NCKX<sup>zydeco</sup>* seizure phenotype was performed. Our results indicate elevation of glial  $\text{Ca}^{2+}$  causes hyperactivation of calcineurin-dependent endocytosis and accumulation of early endosomes. Knockdown of *sandman*, a  $\text{K}_{2\text{P}}$  channel, recapitulates *NCKX<sup>zydeco</sup>* seizures. Restoring glial  $\text{K}^+$  buffering by overexpressing a leak  $\text{K}^+$  channel rescues *zydeco* seizures. These findings indicate cortex glial  $\text{Ca}^{2+}$  couples to  $\text{K}^+$  buffering through calcineurin regulated endo-exocytotic balance and  $\text{K}_{2\text{P}}$  channel expression to modulate neuronal excitability.

## **Introduction**

Glial cells are well known to play structural and supportive roles for their more electrically excitable neuronal counterparts. However, growing evidence indicates glial  $\text{Ca}^{2+}$  signaling influences neuronal physiology on a rapid time scale. In the cortex, glia and neurons exist in equal abundance (Azevedo et al., 2009) and are intimately associated. A single astrocytic glia contacts multiple neuronal cell bodies, hundreds of neuronal processes, and tens of thousands of synapses (Halassa et al., 2007; Ventura and Harris, 1999). Cultured astrocytes oscillate intracellular  $\text{Ca}^{2+}$  spontaneously (Takata and Hirase, 2008) and in response to neurotransmitters (Agulhon et al., 2008; Lee et al., 2010), including glutamate (Cornell-Bell et al., 1990). Glutamate released during normal synaptic transmission is sufficient to induce astrocytic  $\text{Ca}^{2+}$  oscillations (Dani et al., 1992; Wang et al., 2006), which trigger  $\text{Ca}^{2+}$  elevation in co-cultured neurons (Nedergaard, 1994; Parpura et al., 1994) that can elicit action potentials (Angulo et al., 2004; Fellin et al., 2006; Fellin et al., 2004; Pirttimaki et al., 2011). These astrocyte-neuron interactions suggest abnormally elevated glial  $\text{Ca}^{2+}$  might produce neuronal hypersynchrony. Indeed, increased glial activity is associated with abnormal neuronal excitability (Wetherington et al., 2008), and pathologic elevation of glial  $\text{Ca}^{2+}$  can play an important role in the generation of seizures (Gomez-Gonzalo et al., 2010; Tian et al., 2005). However, the molecular pathway(s) by which glia-to-neuron communication alters neuronal excitability is poorly characterized. In addition, how glia interface with synaptic versus non-synaptic regions of neurons is unclear.

All major CNS glial subtypes interact closely with neuronal cell bodies. Protoplasmic astrocytes form extensive contacts on neuronal cell bodies (Allen and Barres, 2009); satellite microglia form contacts between their cell bodies and those of neurons (Baalman et al., 2015); and specialized groups of perineuronal oligodendrocytes reside on neuronal cell bodies (Battefeld et al., 2016; Takasaki et al., 2010). While significant progress has been made in characterizing the contacts between glial cells and axons and synapses, less is understood of the signaling events between any type of glial process and neuronal cell bodies. In this regard, *Drosophila* provides an ideal system to study glial-neuronal soma interactions as the CNS is compartmentalized into two primary regions: the cell cortex (consisting of neuronal cell bodies and their proximal axons) and the synaptic neuropil (containing all CNS neurites and synapses). Two specialized astrocyte-like glial subtypes, astrocytes and cortex glia, are compartmentalized into these brain regions. Astrocytes extend processes that are confined to the neuropil and associate with synapses, axons, and dendrites (Stork et al., 2014). *Drosophila* astrocytes are similar to mammalian protoplasmic astrocytes in terms of their morphology, tiling behavior, expression profiles, and functions in synapse formation (Muthukumar et al., 2014; Stork et al., 2014), synaptic pruning (Tasdemir-Yilmaz and Freeman, 2014), and regulation of synaptic function (Ma et al., 2016). Cortex glia, in contrast, are restricted to the cell cortex region that is devoid of synapses (Awasaki et al., 2008; Poreanu et al., 2005). Cortex glia extend fine processes into the cell cortex region and encapsulate virtually every neuronal cell body in the CNS (Awasaki et al., 2008) (Fig. S1A). Given these tight associations, cortex glia are thought to provide metabolic support and key nutrients to neurons (Volkenhoff et al., 2015). In addition, cortex glia have been shown to exhibit local microdomain  $\text{Ca}^{2+}$  transients close to neuronal cell bodies that may regulate their function (Melom and Littleton, 2013). However, the role of cortex glia in modulating neuronal activity is unclear.

Previous work in our lab identified zydeco (*zyd*), a cortex glial enriched  $\text{Na}^+\text{Ca}^{2+}\text{K}^+$  (NCKX) exchanger involved in maintaining normal neural excitability. Mutations in *NCKX*<sup>zydeco</sup> (hereafter referred to as *zyd*) predispose animals to temperature-sensitive seizures and result in bang sensitivity (seizures induced following a brief vortex). Basal intracellular  $\text{Ca}^{2+}$  levels are elevated in *zyd* cortex glia, while near-membrane microdomain  $\text{Ca}^{2+}$  oscillations observed in wildtype cortex glia are abolished. These findings indicate disruption of glial  $\text{Ca}^{2+}$  regulation triggers enhanced seizure susceptibility. To determine how cortex glial  $\text{Ca}^{2+}$  signaling regulates neuronal

excitability, we took advantage of the *zyd* mutation and performed an RNAi screen for modifiers of the seizure phenotype. Here we show that chronic elevation of glial  $\text{Ca}^{2+}$  causes hyperactivation of calcineurin-dependent endocytosis leading to an endo-exocytosis imbalance. In addition, sandman, a  $\text{K}_{2\text{P}}$  channel, recapitulates *zyd* seizures when knocked down and acts downstream of calcineurin in cortex glia. Sandman was previously identified as the key  $\text{K}^+$  channel that cycles to and from the plasma membrane in a group of central complex neurons to modulate their excitability and control sleep homeostasis in the *Drosophila* circadian pathway (Pimentel et al., 2016). Our findings suggest similar regulation of sandman in cortex glia could allow dynamic control of  $\text{K}^+$  levels surrounding neuronal somas as a mechanism to gate neuronal excitability. Indeed, overexpression of a constitutively active  $\text{K}^+$  channel in cortex glia can rescue *zyd* seizures. Together, these findings suggest glial  $\text{Ca}^{2+}$  interfaces with calcineurin-dependent endocytosis to regulate plasma membrane protein levels and the  $\text{K}^+$  buffering capacity of glia associated with neuronal somas. Disruption of these pathways leads to enhanced neuronal excitability and seizures, suggesting potential targets for future glial-based therapeutic modifiers of epilepsy.

## Results

### **Mutations in a cortex glial NCKX generate stress-induced seizures without affecting brain structure or baseline neuronal function**

We previously identified and characterized a *Drosophila* temperature-sensitive (TS) mutant termed *zydeco* (*zyd*) that exhibits seizures when exposed to a variety of environmental stressors, including heat-shock and acute vortex (Melom and Littleton, 2013). The *zyd* mutation maps to a NCKX exchanger that extrudes cytosolic  $Ca^{2+}$ . Restoring *zyd* function specifically in cortex glial completely reverses the *zyd* seizure phenotype. Cortex glia exhibit spatial segregation reminiscent of mammalian astrocytes, with each glial cell ensheathing multiple neuronal somas (Awasaki et al., 2008; Melom and Littleton, 2013). However, little is known about their role in the mature nervous system. *In vivo*  $Ca^{2+}$  imaging using a myristoylated  $Ca^{2+}$  sensitive-GFP (myrGCaMP5) revealed small, rapid cortex glial  $Ca^{2+}$  oscillations in wildtype *Drosophila* larvae. In contrast, *zyd* mutants lack microdomain  $Ca^{2+}$  transients and exhibit elevated baseline intracellular  $Ca^{2+}$ , indicating altered glial  $Ca^{2+}$  regulation underlies seizure susceptibility in *zyd* mutants (Melom and Littleton, 2013).

Given cortex glia regulate the guidance of secondary axons and maintenance of cortical structural integrity (Coutinho-Budd et al., 2017; Dumstrei et al., 2003; Spindler et al., 2009), we first tested whether the *zyd* TS seizure phenotype might arise secondary to developmental changes or defective assembly of brain circuits. We knocked down the protein chronically throughout development or conditionally in adult stages following brain development using a UAS-*zyd*<sup>RNAi</sup> hairpin expressed with a pan-glial driver (*repo-gal4*) or cortex glial-specific drivers (*NP2222-gal4* and *GMR54H02-gal4*). Chronic pan-glial knock down of *zyd* caused lethality, with >95% of animals dying before the 3<sup>rd</sup> instar larval stage (Fig. S1B). In contrast, both chronic and inducible cortex glial knockdowns mimicked the *zyd* TS seizure phenotype (Figs. 1A), suggesting the *zyd* TS phenotype does not arise from a developmental defect. Seizure characteristics, including temperature threshold for seizure initiation and seizure kinetics, were similar between 3<sup>rd</sup> instar larvae and adults (Fig. S1C-D), indicating a comparable requirement for *zyd* at both stages. Morphological examination of brain structure and cortex glial morphology using fluorescent microscopy revealed no apparent changes in *zyd* mutants (Fig. S1E). To determine if loss of *zyd* affected glial or neuronal cell survival, we quantified the cell death marker DCP-1 (cleaved death caspase protein-1 (Akagawa et al., 2015)) in control and *zyd* 3<sup>rd</sup> instar larvae and adults. No change in cleaved DCP1 levels were found, indicating basal cell death was unaffected (Fig. S1F). Together, these results suggest that the *zyd* TS seizure phenotype is not due to morphological or developmental changes in brain anatomy, or changes in the ability of cortex glia to ensheath neuronal cell bodies.

We next assayed if *zyd* animals displayed aberrant behaviors or altered neuronal excitability in the absence of the elevated temperature trigger or acute vortex needed to induce seizures in the mutant. Astrocytic  $Ca^{2+}$  activity has been correlated with elevated arousal in awake mice (Ding et al., 2013; Paukert et al., 2014; Srinivasan et al., 2015) and in *Drosophila* (Ma et al., 2016). We therefore used a touch assay (Ma et al., 2016; Zhou et al., 2012) to investigate the role of altered cortex glial  $Ca^{2+}$  signaling in larval startle-induced behaviors. Crawling larvae touched anteriorly respond by pausing and continuing forward (type I response) or moving backward with an escape response (type II response). We found that wildtype, *zyd* and *NP2222>zyd*<sup>RNAi</sup> larvae exhibited similar frequencies of type I and type II responses (Fig. S1G). In addition, adult *zyd* flies exhibited normal locomotion (Fig. S1H) and larvae exhibited normal light avoidance responses at room temperature (Fig. S1I), indicating baseline neuronal properties required for these behaviors are unaffected.

To directly measure changes in neuronal excitability that might contribute to *zyd* seizures, we performed electrophysiological recordings in the giant fiber system (GFS, (Pavlidis and Tanouye, 1995)). In this assay, GF neurons are stimulated in the adult brain and the output

response is recorded. By progressively increasing stimulation intensity, the voltage threshold that triggers seizure activity in the GF circuit can be directly assayed, providing a readout of neuronal excitability. Most *Drosophila* bang-sensitive mutations display seizure induction at much lower voltages, consistent with their primary effect on membrane excitability thresholds within the neuron. For example, *para*<sup>bss1</sup>, a gain-of-function bang sensitive mutation in the voltage-gated Na<sup>+</sup> channel, dramatically lowers seizure threshold (Fig. 1B) (Parker et al., 2011). In contrast, the voltage threshold for seizure induction in *zyd* was not significantly different from controls (Fig. 1B), indicating basic intrinsic neuronal properties are not altered in *zyd* animals at rest. To determine if elevated neuronal activity is required for the stress-induced seizures in *zyd* mutants, we assayed seizure behavior in animals with reduced synaptic transmission and neuronal activity. Pan-neuronal knockdown of Cacophony (*cac*), the presynaptic voltage-gated Ca<sup>2+</sup> channel responsible for neurotransmitter release (Kawasaki et al., 2004; Rieckhof et al., 2003), significantly reduced neuronal activity (Fig. S1J) and rescued *zyd* TS-induced seizures (Fig. 1C). These findings indicate elevated neuronal activity in *zyd* mutants during the heat shock is required for seizure induction following dysregulation of cortex glial Ca<sup>2+</sup>.

### **A genetic modifier screen of the *zyd* seizure phenotype reveals glia to neuron signaling mechanisms**

To elucidate pathways by which cortex glial Ca<sup>2+</sup> signaling controls somatic regulation of neuronal function and seizure susceptibility, we performed a targeted RNAi screen for modifiers of the *zyd* TS seizure phenotype in adult animals. We reasoned that removal of a gene product required for this signaling pathway would prevent *zyd* TS seizures when absent. We used the pan-glial driver *repo-gal4* to express RNAi to knockdown 847 genes encoding membrane receptors, secreted ligands, ion channels and transporters, vesicular trafficking proteins and known cellular Ca<sup>2+</sup> homeostasis and Ca<sup>2+</sup> signaling pathway components (Tables S1, S2). The screen revealed multiple genetic interactions, identifying gene knockdowns that completely (28) or partially (21) rescued *zyd* seizures, caused lethality on their own (95) or synthetic lethality in the presence of *zyd* (5), enhanced *zyd* seizures (37) or triggered seizures (3) in a wildtype background (Fig. 1D, Table S1). Given the broad role of Ca<sup>2+</sup> as a regulator of intracellular biology, we expected elevated Ca<sup>2+</sup> levels in *zyd* mutants to interface with several potential glial-neuronal signaling mechanisms. Indeed, the screen identified multiple candidates controlling glial-to-neuron communication, including regulators of vesicular trafficking, neurotransmitter receptors and ion channels, and Ca<sup>2+</sup> effector proteins that suppress *zyd* seizures when knocked down specifically in glia (Fig. 1D, Table S1).

Beyond regulators of the *zyd* phenotype, the screen also identified Stim (stromal interaction molecule), an ER Ca<sup>2+</sup> sensor for store operated Ca<sup>2+</sup> entry (SOCE), as a key Ca<sup>2+</sup> signaling component involved in TS seizure generation. Knockdown of Stim in wildtype adult animals caused seizures that were similar to those observed in *zyd* mutants (Fig. 1E), suggesting defects in glial microdomain Ca<sup>2+</sup> (*zyd*) or the SOCE pathway both increase neuronal seizure susceptibility. Recordings of motor central pattern generator (CPG) output at the larval neuromuscular junction (NMJ) showed that Stim<sup>RNAi</sup> larvae exhibit rapid, unpatterned firing at 38°C, similar to *zyd* mutants, whereas wildtype larvae retain motor neuron bursting necessary for normal crawling behavior (Fig. 1F). To determine if these distinct Ca<sup>2+</sup> entry pathways impinged on a similar mechanism for seizure induction, we tested genetic interaction between SOCE defects and *zyd* mutants. If both Ca<sup>2+</sup> entry mechanisms impinged on the same pathway, they should not show synergistic interactions when both are disrupted. However, knockdown of Stim in the *zyd* background enhanced *zyd* seizures (Fig. 1E), indicating additive effects and suggesting Ca<sup>2+</sup> is likely to interface with distinct glial-neuronal pathways depending upon the source and location of aberrant Ca<sup>2+</sup> signaling. Indeed, *zyd*-dependent seizures require calcineurin function, while SOCE pathway dysfunction does not (see below). Distinctions between microdomain and

ER-dependent  $\text{Ca}^{2+}$  signaling pathways have been previously observed in mammals as well (Bindocci et al., 2017; Savtchouk and Volterra, 2018).

Given TS seizures in *zyd* mutants can be fully rescued by reintroducing the wildtype *zyd* (NCKX) protein in cortex glia, we expected the genes identified in the RNAi pan-glia knockdown screen to function specifically within this population of cells. To directly examine cell-type specificity of the suppressor hits, the RNAi screen was repeated with drivers restricted to either astrocyte or cortex glial subtypes (Alrm-gal4 for astrocytes and NP2222-gal4 and GMR54H02-gal4 for cortex glia, Fig. 1D, Table S1). For the majority of suppressors, rescue with the glial-subtype specific drivers was weaker, likely due to lower RNAi expression levels compared to the stronger repo-gal4 driver line (Fig. 1D). In several cases (*nompC*, *Nmdar2*), however, near complete rescue of the *zyd* seizure phenotype could be achieved when the gene was knocked down using the astrocyte driver Alrm-gal4 (Fig. 1D). This surprising observation indicates that although seizure induction in *zyd* mutants arises from abnormal  $\text{Ca}^{2+}$  signaling within cortex glia, normal astrocyte function is required for either the propagation or maintenance of the subsequent excitability changes that drive the TS seizure phenotype. We recently discovered that *Drosophila* astrocytes employ  $\text{Ca}^{2+}$ -mediated signaling pathways to dynamically regulate the surface levels of the GABA transporter, GAT, which negatively controls neuronal activity through modulation of synaptic GABA levels (Zhang et al., 2017). Together with the RNAi suppressor screen hits that function within astrocytes, these data indicate astrocytes regulate the seizure-inducing defects arising in cortex glia in the *zyd* mutant. For the remaining analysis, we focused on the characterization of the cortex glial  $\text{Ca}^{2+}$ -dependent pathway that is mis-regulated in *zyd*, and how this mis-regulation promotes neuronal seizure susceptibility.

### **Cortex glial calcineurin activity is required for seizures in *zyd* mutants**

We previously observed that knockdown of glial calmodulin (Cam) eliminates the *zyd* seizure phenotype (Melom and Littleton, 2013), suggesting a  $\text{Ca}^{2+}$ /Cam-dependent signaling pathway regulates glial to neuronal communication. Cam is an essential  $\text{Ca}^{2+}$ -binding protein that regulates multiple  $\text{Ca}^{2+}$ -dependent cellular processes and is abundantly expressed in *Drosophila* glia (Altenhein et al., 2006), although its role in glial biology is unknown. Calcineurin (CN) is a highly conserved  $\text{Ca}^{2+}$ /Cam-dependent protein phosphatase implicated in a number of cellular processes in mammals (Rusnak and Mertz, 2000). In the RNAi screen for *zyd* interactors, pan-glia knockdown of the regulatory CN B subunit, CanB2, completely rescued both heat-shock and vortex induced seizures in *zyd* animals (Fig. 1D, 2A-C). In contrast to the continuous neuronal firing observed in *zyd* mutants, CPG recordings demonstrated that *zyd*;repo>CnB2<sup>RNAi#1</sup> larvae exhibit normal rhythmic firing at 38°C similar to controls (Fig. 2B). Similar results were observed using three additional, non-overlapping CanB2 RNAi constructs (Fig. 2A, 2F). To refine the glial subpopulation in which CanB2 activity is necessary to promote seizures in *zyd* mutants, we knocked CanB2 down using different glial drivers. CanB2 knockdown in astrocytes resulted in no rescue of the *zyd* phenotype (Fig. 1D). CanB2 knockdown with a cortex-glia specific driver (NP2222) greatly improved the *zyd* phenotype. Animals no longer displayed continuous seizures, but the rescue was less robust compared to pan-glia knockdown, likely due to lower expression of the RNAi (Fig. 2D, Fig. S2A). Indeed, rescue was greatly enhanced by cortex glial-specific knockdown of CanB2 using two copies of the CanB2 RNAi construct (Fig. 2D), with ~90% of *zyd*;NP2222>CanB2<sup>2xRNAi</sup> adult animals lacking seizures. The effect of CanB2 knockdown was specific to cortex glia, as it was insensitive to blockade of expression of the CanB2 RNAi in neurons using C155-gal80 (a neuron specific gal4 repressor; Fig. 2D and S2A). To exclude a developmental effect of CanB2 knockdown within glia, we blocked gal4/UAS-driven CanB2<sup>RNAi</sup> with gal80<sup>ts</sup> and expressed a single copy of CanB2<sup>RNAi</sup> only in adult *zyd* mutants. Adult flies reared at the permissive temperature for gal80<sup>ts</sup> to allow CanB2<sup>RNAi</sup> expression exhibited significantly less seizures after 3 days, with only ~20% of flies displaying *zyd*-like seizures by 5 days (Fig. 2E). *Zyd* seizure rescue by CanB2 knockdown did not result from simple alterations in motility, as

repo>CanB2<sup>RNAi</sup> and *zyd*;repo>CanB2<sup>RNAi</sup> animal exhibited normal larval light avoidance responses (Fig. S2B) and adult locomotion (Fig. S2C). In contrast to rescue of the *zyd* phenotype, CanB2 knockdown could not rescue TS seizures induced by increasing glial Ca<sup>2+</sup> through overexpression of the Ca<sup>2+</sup> channel TRPA (Fig S2D) or RNAi knockdown of Stim (Fig. S2E), indicating glial-triggered seizures in these genetic backgrounds employ distinct Ca<sup>2+</sup>-regulated pathways to alter neuronal excitability. We conclude that CanB2 is required in cortex glia to promote *zyd* TS seizure activity.

CN is a heterodimer composed of a ~60 kDa catalytic subunit (CanA) and a ~19 kDa EF-hand Ca<sup>2+</sup>-binding regulatory subunit (CanB). Both subunits are essential for CN phosphatase activity. Previous studies in *Drosophila* demonstrated several CN subunits (*CanA-14F*, *CanB*, and *CanB2*) are broadly expressed in the adult *Drosophila* brain (Tomita et al., 2011) and that neuronal CN is essential for regulating sleep (Nakai et al., 2011; Tomita et al., 2011). CN function within glia has not been characterized. The *Drosophila* genome contains three genes encoding CanA (CanA1, Pp2B-14D and CanA-14F) and two genes encoding CanB (CanB and CanB2) (Takeo et al., 2006). We found that pan-glial knockdown of two CanA subunits, Pp2B-14D and CanA-14F, partially rescued *zyd* heat-shock and vortex induced seizures (Fig. 2C, F). The rescue was more robust for vortex-induced seizures than those induced by heat-shock, suggesting heat-shock is likely to be a more severe hyperexcitability trigger. Rescue was enhanced by knockdown of both Pp2B-14D and CanA-14F (Fig. 2G), with more than ~90% of *zyd*;repo>2xCanA<sup>RNAi</sup> flies lacking seizures, suggesting a redundant function of these two subunits in glial cells. To further verify the effect of CanA knockdown and the glial subpopulation in which CN activity is required, we overexpressed a dominant negative (DN) form of CanA (Pp2B-14D<sup>H217Q</sup>) using either pan-glial (repo-gal4) or two different cortex-glial specific drivers (NP2222-gal4 and GMR54H02-gal4). Overexpressing Pp2B-14D<sup>H217Q</sup> resulted in ~50% of *zyd*;Pp2B-14D<sup>H217Q</sup> flies becoming seizure-resistant, regardless of the driver used (Fig 2H). Imaging of intracellular Ca<sup>2+</sup> in cortex glia with GMR54H02-gal4 driven myrGCaMP6s revealed that CN knockdown had no effect on either the elevated basal Ca<sup>2+</sup> levels or the lack of microdomain Ca<sup>2+</sup> events observed in *zyd* cortex glia (Fig. 2I-J). These observations indicate CN function is required downstream of elevated intracellular Ca<sup>2+</sup>, rather than to regulate Ca<sup>2+</sup> influx or efflux in cortex glial cells. Together, these results demonstrate that a CN-dependent signaling mechanism in cortex glia is required for glial-neuronal communication that drives seizure generation in *zyd* mutants.

### **Calcineurin activity is enhanced in *zyd* cortex glia**

To characterize CN activity in wildtype and *zyd* cortex glia we used the CalexA system as a reporter for CN activity. CalexA (Ca<sup>2+</sup>-dependent nuclear import of LexA) (Masuyama et al., 2012) was originally designed for labeling active neurons in behaving animals. In this system, sustained neural activity induces CN activation and dephosphorylation of a chimeric transcription factor LexA-VP16-NFAT (termed CalexA) which is then transported into the nucleus. The imported dephosphorylated CalexA drives GFP reporter expression in active neurons (for schematic representation, see Fig. S2F). The CalexA components were brought into control and *zyd* mutant backgrounds to directly assay CN activity. A substantial basal activation of CN was observed in control 3<sup>rd</sup> instar larval cortex glia at room temperature using fluorescent imaging (Fig. 3A). CN activity and the resulting GFP expression was enhanced in *zyd* cortex glia (Fig. 3B). Western blot analysis of CalexA-induced GFP expression in adult head extracts revealed enhanced cortex glial CN activity in adult *zyd* mutants compared to controls as well (23 ± 3% enhancement, Fig 3D-E). RNAi knockdown of CanB2 greatly reduced CalexA GFP expression as expected (27 ± 1% reduction, Fig. 3C-E). These results demonstrate CN activity is enhanced downstream of the elevated Ca<sup>2+</sup> levels in *zyd* mutant cortex glia, and that CN activity can be efficiently reduced by RNAi knockdown of CanB2.



### **Pharmacological targeting of the glial calcineurin pathway rescues *zyd* seizures**

Several seizure mutants in *Drosophila* can be suppressed by commonly used anti-epileptic drugs (Kuebler and Tanouye, 2002; Song and Tanouye, 2008), indicating conservation of key mechanisms that regulate neuronal excitability. CN activity is strictly controlled by  $Ca^{2+}$  levels, calmodulin, and CanB, and can be inhibited by the immunosuppressants cyclosporine A (CsA) and FK506. The CN inhibitor FK506 has been previously shown to reduce seizures in a rodent kindling model (Moia et al., 1994; Moriwaki et al., 1996), suggesting CN can modulate epilepsy in mammals. To assay if *zyd* TS seizures can be prevented with anti-CN drugs, adult flies were fed with media containing different anti-CN drugs (CsA, FK506 and CN585 (Erdmann et al., 2010)) and tested for HS induced seizures after 0, 3, 6, 12 and 24 hours of drug feeding (red arrowheads in Fig. 4A, Fig. 4B-C). *Zyd* flies fed with 1 mM CsA for 12 hours showed ~80% less seizures than control (Fig. 4B, C), while two other inhibitors, FK506 and CN585, had much weaker effects (Fig. 4B). Seizure rescue by CsA was dose-dependent, with less robust suppression when flies were fed with 0.3 mM CsA (Fig. 4D-E). The CsA rescue was reversible, as *zyd* seizures reoccurred following 12 hours of CsA withdrawal (Fig. 4C). We conclude that pharmacologically targeting the glial CN pathway can improve the outcome of glial-derived neuronal seizures in the *zyd* mutant.

### **Cortex glial knockdown of the sandman two-pore-domain $K^+$ channel mimics *zyd* seizures**

To explore how CN hyperactivation promotes seizures, we conducted a screen of known and putative CN targets using RNAi knockdown with repo-gal4. We concentrated our screen on putative CN target genes that are involved in signal transduction (Table S3). This screen revealed that pan-glial knockdown of sandman (*sand*), the *Drosophila* homolog of TRESK (KCNK18) and a member of the two-pore-domain  $K^+$  channel family ( $K_{2P}$ ), caused adult flies to undergo TS-induced seizures similar to *zyd* mutants (Fig. 5A). Vortex-induced seizures in repo>*sand*<sup>RNAi</sup> were less severe than those observed in *zyd*, with only ~50% of *sand*<sup>RNAi</sup> flies showing seizures (Fig. S3A). TS-induced seizures in repo>*sand*<sup>RNAi</sup> adults were found to have the same kinetics and temperature threshold as seizures observed in *zyd* mutants (Fig. 5A, B), and CPG recordings showed that repo>*sand*<sup>RNAi</sup> larvae exhibit rapid, unpatterned firing at 38°C, similar to *zyd* mutants (Fig. 5C). Cortex-glial specific knockdown of *sand* recapitulated ~50% of the seizure effect when two copies of the RNAi were expressed (Fig. 5A, B). The less robust effect observed with the cortex-glial driver could be due to less effective RNAi knockdown or secondary to a role for *sand* in other glial subtypes. To determine if *sand* functions in other glia subtypes to mimic the *zyd* seizure pathway, we expressed *sand*<sup>RNAi</sup> using the pan-glial driver repo-gal4 and inhibited expression specifically in cortex glia with GMR54H02>gal80. In the absence of cortex glial-knockdown of *sand*, seizure generation was suppressed (Fig. 5A). Similar to *zyd* mutants, *sand*<sup>RNAi</sup> animals did not show changes in general activity and locomotion at room temperature (Fig. 5D). Finally, unlike the case with Stim removal in the SOCE pathway, RNAi knockdown of *sand* did not enhance the *zyd* phenotype (Fig. S3B), suggesting seizures due to loss of *sand* and *zyd* impinge on a similar pathway.

Mammalian astrocytes modulate neuronal network activity through regulation of  $K^+$  buffering (Bellot-Saez et al., 2017), in addition to their role in uptake of neurotransmitters such as GABA and glutamate (Murphy-Royal et al., 2017). Human  $K_{ir4.1}$  potassium channels (*KCNJ10*) have been implicated in maintaining  $K^+$  homeostasis, with mutations in the loci causing epilepsy (Haj-Yasein et al., 2011). However,  $K_{ir}$  channels are unlikely to be the only mechanism for glial  $K^+$  clearance, as  $K_{ir4.1}$  channels account for less than half of the  $K^+$  buffering capacity of mature hippocampal astrocytes (Ma et al., 2014). To determine if cortex glial  $K_{ir}$  channels regulate seizure susceptibility in addition to *sand*, we used repo-Gal4 to knock down all three *Drosophila*  $K_{ir}$  family members (*Irk1*, *Irk2* and *Irk3*). Pan-glial knockdown of the *Drosophila*  $K_{ir}$  family did not cause seizures (Fig. S3C), while knock down of either *Irk1* or *Irk2* slightly enhanced the *zyd* phenotype (Fig. S3D). Similarly, repo-gal4 knockdown of other well-known *Drosophila*  $K^+$  channels beyond

the  $K_{ir}$  family also did not cause seizures (Fig. S4C), indicating sand is likely to play a preferential role in  $K^+$  buffering in *Drosophila* cortex glia.

The mammalian sand homolog, TRESK, is directly activated by CN dephosphorylation (Czirjak et al., 2004; Enyedi and Czirjak, 2015), while *Drosophila* sand was shown to be modulated in sleep neurons by activity-induced internalization from the plasma membrane (Pimentel et al., 2016). Regardless of the mechanism by which CN may regulate the protein, we hypothesized that sand is epistatic to CN in controlling *zyd*-mediated seizures. Indeed, inhibition of CN by RNAi or CsA did not alter sand<sup>RNAi</sup>-induced seizures (Fig. 5E), placing sand downstream of CN activity. Furthermore, knockdown of sand in the *zyd* background does not alter the elevated basal  $Ca^{2+}$  or the lack of microdomain  $Ca^{2+}$  events in *zyd* mutants (Fig. 5F, G), suggesting sand is downstream to the abnormal  $Ca^{2+}$  signaling in *zyd*. Overall, these findings suggest elevated  $Ca^{2+}$  in *zyd* mutants leads to hyperactivation of CN and subsequent reduction in sand function. These results suggest that impairment in glial buffering of the rising extracellular  $K^+$  during elevated neuronal activity and stress conditions (i.e. heat shock or acute vortex) causes enhanced seizure susceptibility in *zyd* mutants.

### **Enhanced endocytosis in *zyd* cortex glia**

We next sought to examine how elevated CN activity in *zyd* mutants alters sand function. The mammalian sand homolog, TRESK, is constitutively phosphorylated on four serine residues (S264 by PKA, and S274, S276 and S279 by MARK1) (Enyedi and Czirjak, 2015). Two of these residues are conserved in *Drosophila* sand (S264 and S276, see Fig. S3E for protein alignment). Constitutive dephosphorylation and subsequent activation of sand by CN would be predicted to increase  $K^+$  buffering following hyperactivation of the nervous system by stressors, and thus less seizure activity would be expected – opposite to what we have observed. If this regulatory mechanism is active in *Drosophila* cortex glia, we hypothesized that knockdown of either PKA or Par-1 (the *Drosophila* MARK1 homolog) would lead to enhanced activity of sand and improvement or rescue of *zyd* seizures. However, neither pan-glial or cortex glial knockdown of either kinase (PKA-C1, PKA-C2, PKA-C3 and Par-1), or overexpression of a PKA inhibitory peptide (PKI), altered the *zyd* phenotype (Table S4). Together with the prediction that regulation of sand by dephosphorylation should lead to seizure suppression, these results argue against enhanced sand dephosphorylation as the primary cause of *zyd* seizures.

A second mechanism to link CN hyperactivation to sand regulation is suggested by a previous study demonstrating sand expression on the plasma membrane of neurons involved in sleep homeostasis is regulated by activity-dependent internalization (Pimentel et al., 2016). Cam and CN activate several endocytic  $Ca^{2+}$  sensors and effectors that control  $Ca^{2+}$ -dependent endocytosis (Xie et al., 2017). If hyperactivity of CN leads to enhanced internalization of sand and subsequent seizure susceptibility due to decreased  $K^+$  buffering capacity, interrupting cortex glial endocytosis should suppress *zyd* seizures. To test this model, we used cortex glial-specific RNAi to knock down genes involved in endocytosis and early endosomal processing and trafficking. Cortex glial knockdown of several essential endocytosis genes, including dynamin-1 and clathrin heavy and light chains, caused embryonic lethality. In contrast, cortex glial knockdown of Rab5, a Rab GTPase regulator of early endosome (EE) dynamics (Langemeyer et al., 2018), and Endophilin A (EndoA), a BAR-domain protein involved in early stages of endocytosis (Verstreken et al., 2002), completely suppressed *zyd* TS seizures (Fig. 6A). A second, non-overlapping hairpin and a dominant negative (DN) construct for Rab5 (Rab5<sup>DN</sup>) resulted in early larval lethality (Table S5), likely due to more efficient Rab5 activity suppression. However, conditionally expressing Rab5<sup>DN</sup> in adult cortex glia partially rescued *zyd* seizures (Fig. 6B). Rab5 is engaged in the initial step of vesicle endocytosis and recycling (Dunst et al., 2015), suggesting a key role for this process in regulating glial-to-neuronal soma signaling. To determine if the observed rescue was specifically associated with early endocytosis defects, we assayed seizure suppression in *zyd* mutants following knockdown of the entire family of *Drosophila* Rab GTPases, most of which are

expressed in *Drosophila* cortex glia (Coutinho-Budd et al., 2017). Beyond Rab5, none of the remaining Rab proteins altered the *zyd* seizure phenotype or caused a behavioral phenotype on their own following RNAi-mediated knockdown (Table S5).

To assay if excess endocytosis secondary to CN hyperactivity disrupts membrane trafficking, we imaged endosomal compartments by expressing GFP-tagged Rab proteins in cortex glial cells of control and *zyd* animals. We found that large (>0.1  $\mu\text{m}^2$ ) Rab5-positive early endosomes accumulated in *zyd* cortex glia compared to controls (Fig. 6C). Feeding *zyd* larvae the CN inhibitor, CsA (1 mM), restored the number of Rab5 compartments to control levels (Fig. 6D). These results indicate CN hyperactivation secondary to elevated  $\text{Ca}^{2+}$  levels in *zyd* mutants increases endocytosis and the formation of early endosomes in cortex glia.

### **Chronic inhibition of dynamin-mediated endocytosis rescues *zyd* seizures**

Our previous analysis of the *zyd* mutant indicated that basal intracellular  $\text{Ca}^{2+}$  is elevated in cortex glia, with  $\text{Ca}^{2+}$  levels increasing even more when *zyd* animals are heat-shocked (Melom and Littleton, 2013). This additional elevation in  $\text{Ca}^{2+}$  could potentially further enhance CN activity and endocytosis beyond that observed at rest. These data raise the question of whether the basal enhancement of endocytosis or the additional heat shock-induced  $\text{Ca}^{2+}$  increase is the primary cause for seizure susceptibility in *zyd* mutants. To test these two models, we conditionally manipulated endocytosis by overexpressing a TS dominant-negative form of Dynamin-1 ( $\text{Shi}^{\text{ts}}$ ) in *zyd* cortex glia. This mutant version of Dynamin has normal activity at room temperature and a dominant-negative function upon exposure to the non-permissive temperature (>29°C, Fig. 6F). Acute inhibition of endocytosis by inactivation of  $\text{Shi}^{\text{ts}}$  in cortex glia did not suppress *zyd* seizures, suggesting further enhancement of CN activity and endocytosis specifically during the heat shock is not likely to be the cause of the rapid-onset seizures observed in *zyd* mutants. Given the chronic enhancement in CN activity and endocytosis in *zyd* mutants demonstrated by enhanced CalnexA signaling (Fig. 3) and early endosome accumulation (Fig. 6C-D), we hypothesized that inhibiting endocytosis prior to exposing animals to a heat shock might improve their phenotype by altering the plasma membrane protein content over longer timescales. We incubated *zyd;NP2222>Shi<sup>ts</sup>* flies at a non-permissive temperature for  $\text{Shi}^{\text{ts}}$  (31°C) for either 3 or 6 hours, and then tested for heat shock-induced seizures at 38.5°C (Fig. 6E-F). *Zyd* mutants alone do not undergo seizures at 31°C, nor does pre-incubation at 31°C alter the subsequent seizure phenotype observed at 38.5°C. In contrast, inhibition of endocytosis for 6 hours at 31°C in *zyd* mutants co-expressing  $\text{Shi}^{\text{ts}}$  suppressed the subsequent seizures observed during a 38.5°C heat shock in ~80% of animals (Fig. 6F). A shorter 3 hour inhibition did not cause a significant improvement in seizures. The seizure suppression observed after 6 hours of Dynamin inhibition was reversible, as adults tested 12 or 24 hours after return to room temperature regained the *zyd* seizure phenotype (Fig. 6G). We conclude that chronic hyperactivation of CN and endocytosis caused by elevated basal  $\text{Ca}^{2+}$  in *zyd* cortex glia is the primary cause for *zyd* seizures.

### **Increasing glial $\text{K}^+$ uptake rescues *zyd*-dependent seizures**

Genetic analysis of the *zyd* mutant indicate the primary cause of seizure susceptibility is chronic enhancement in  $\text{Ca}^{2+}$ -dependent CN activity and subsequent increases in endocytosis in cortex glia. We hypothesize this enhancement in endocytosis leads to increased internalization of plasma membrane proteins such as  $\text{K}^+$  channels, which in turn disrupt  $\text{K}^+$  uptake and buffering by cortex glial cells during periods of intense activation of the nervous system (Fig. 7A). To test this model further, we assayed if artificially increasing cortex glial  $\text{K}^+$  uptake in *zyd* mutants by overexpressing another  $\text{K}^+$  leak channel could suppress the seizure phenotype. Indeed, constitutive cortex glial overexpression of the open  $\text{K}^+$  channel EKO (White et al., 2001) rescued vortex-induced seizures in ~75% of *zyd* mutants (Fig. 7B). During a heat shock, cortex glial overexpression of EKO led to a dramatic change in the behavior of ~60% of *zyd* animals, changing the seizure phenotype to hypoactivity or complete paralysis (Fig. 7C). CPG recordings revealed

that *zyd*;repo>EKO larvae lose all bursting and normal CPG activity at 38°C (Fig. 7D, middle), while *zyd*;NP2222>EKO regain normal wildtype-like rhythmic activity (Fig. 7D, right). These results indicate cortex glial K<sup>+</sup> buffering is critical for neuronal excitability during states of intense excitation as observed following heat shock or acute vortex. During these periods of intense neuronal activity in *zyd* mutants, defective cortex glial K<sup>+</sup> buffering surrounding neuronal somas leads to seizures. Enhancing K<sup>+</sup> buffering can either reverse the seizure phenotype or push the scales toward neuronal hypo-excitability and paralysis. Future studies will be required to determine if sand function is dynamically modulated by normal microdomain Ca<sup>2+</sup> oscillatory activity in wildtype cortex glia in response to changes in neuronal activity, which would provide a robust glial-based homeostatic mechanism to maintain neuronal spiking rates in acceptable ranges.

## Discussion

Significant progress has been made in understanding glial-neuronal communication at synaptic and axonal contacts, but whether glia regulate neuronal function via signaling at somatic regions remains largely unstudied. A single mammalian astrocyte can be associated with multiple neuronal cell bodies and thousands of synapses, making it challenging to direct manipulations that alter glial signaling only at neuronal somas. *Drosophila* cortex glia ensheath multiple neuronal soma but do not contact synapses (Awasaki et al., 2008). These tight associations with neuronal cell bodies make cortex glial an ideal system to explore how glia regulate neuronal function at the soma. In this study, we took advantage of the *zydeco* TS seizure mutation in a NCKX Ca<sup>2+</sup> exchanger to explore pathways by which cortex glial cells regulate neuronal excitability. We found that elevation of basal Ca<sup>2+</sup> levels in cortex glia leads to hyperactivation of Ca<sup>2+</sup>-CN dependent endocytosis. Seizures in *zyd* mutants can be fully suppressed by either conditional inhibition of endocytosis or by pharmacologically reducing CN activity. Two well-characterized mechanisms by which glia regulate neuronal excitability and seizure susceptibility are neurotransmitter uptake via surface transporters and spatial K<sup>+</sup> buffering. Cortex glia do not contact synapses, making it unlikely they are exposed to neurotransmitters. Instead, cortex glial-knockdown of the two-pore K<sup>+</sup> channel (K<sub>2P</sub>) sandman, the *Drosophila* homolog of TRESK/KCNK18, recapitulates *zyd* TS seizures. These findings suggest impairment in K<sup>+</sup> buffering during hyperactivity in *zyd* mutants underlies the increased seizure susceptibility, providing an unexpected link between glial Ca<sup>2+</sup> signaling and K<sup>+</sup> buffering. Consistent with this model (Fig. 7A), enhancing cortex glial K<sup>+</sup> uptake by overexpressing a constitutively open K<sup>+</sup> channel (EKO (White et al., 2001)) reduces neuronal activity in *zyd* mutants, rescues vortex-induced seizures, and reverses the TS behavioral phenotype from seizures to paralysis.

Astrocytes, as well as other glial subtypes, exhibit dynamic fluctuations in intracellular Ca<sup>2+</sup> *in vitro* (Fatatis and Russell, 1992; Nett et al., 2002) and *in vivo* (Nimmerjahn et al., 2009; Porter and McCarthy, 1996). Despite decades of studies on astrocytic Ca<sup>2+</sup> activity, signaling pathways underlying these transients and their *in vivo* relevance to brain activity are poorly defined and controversial (Fiacco and McCarthy, 2018; Savtchouk and Volterra, 2018). Prior studies examining astrocytic Ca<sup>2+</sup> signaling used several approaches to artificially increase intracellular Ca<sup>2+</sup> (transgenic receptor expression, caged Ca<sup>2+</sup> photolysis and pharmacological or optogenetic stimulation) (Savtchouk and Volterra, 2018). However, it is unclear if these methods mimic physiological astrocytic responses and how these manipulations alter *in vivo* behavior (Agulhon et al., 2010; Fiacco et al., 2007; Wang et al., 2012a; Wang et al., 2012b). Likewise, the distinction between signaling events mediated by local microdomain Ca<sup>2+</sup> oscillatory activity that require extracellular Ca<sup>2+</sup> entry versus the more well-studied IP<sub>3</sub>-dependent release of Ca<sup>2+</sup> from ER stores has only been recently appreciated (Bindocci et al., 2017; Fiacco and McCarthy, 2018; Savtchouk and Volterra, 2018). The *Drosophila zyd* mutation was identified in an unbiased genetic screen for behavioral mutants that triggered TS-dependent seizures, thus establishing the biological importance of the pathway before the gene mutation and cellular origin of the defect

was known. The elevation in cortex glial  $\text{Ca}^{2+}$  levels found in *zyd* mutants provides a mechanism to explore how this pathway influences neuronal excitability. While we focused on CN-dependent endocytosis and  $\text{K}^+$  buffering by cortex glial cells in *zyd* animals, our study uncovered evidence for additional pathways by which glia modulate neuronal excitability as well. Knockdown of Stim in glia, a key regulator of SOCE, also caused TS seizures but did not require CN activity, suggesting glia possess more than one  $\text{Ca}^{2+}$ -sensitive pathway that regulates neuronal excitability. In addition, we found evidence that astrocyte-like glia modulate the expression of seizures that arise from elevated  $\text{Ca}^{2+}$  signaling within cortex glia, as several RNAi suppressor hits rescue *zyd* seizures when knocked down using an astrocyte-specific driver. We recently found that  $\text{Ca}^{2+}$  elevation in astrocyte-like glia results in the rapid internalization of the astrocytic plasma membrane GABA transporter GAT and subsequent silencing of neuronal activity through elevation in synaptic GABA levels (Zhang et al., 2017). As such,  $\text{Ca}^{2+}$ -regulated endo/exocytic trafficking of neurotransmitter transporters and  $\text{K}^+$  channels to and from the plasma membrane may represent a broadly used mechanism for linking glial  $\text{Ca}^{2+}$  activity to the control of neuronal excitability at synapses and cell bodies, respectively.

CN is the only  $\text{Ca}^{2+}$ /Cam-dependent phosphatase encoded in the genome and is highly expressed throughout the brain (Furman and Norris, 2014; Goto et al., 1986a, b; Kuno et al., 1992; Polli et al., 1991). CN interacts with numerous neuronal substrates to modulate diverse functions, including receptor and ion channel trafficking, ion channel function and gene regulation (Baumgartel and Mansuy, 2012). Neuronal CN also controls synapse loss, dendritic atrophy, synaptic dysfunction, and neuronal vulnerability (Abdul et al., 2010; Reese and Tagliatela, 2011). In contrast, astrocytic CN expression has been shown to increase during aging, injury and disease. Glial cells rely on CN signaling pathways to regulate phenotypic switching/cellular activation, immune-like responses and cytokine production (Furman and Norris, 2014), with the pathway being intimately involved in neuroinflammation (Furman and Norris, 2014; Kataoka et al., 2009; Nagamoto-Combs and Combs, 2010; Rojanathammanee et al., 2013; Shiratori et al., 2010). The role of CN in astrocytes during normal brain states is unclear (Chen et al., 2016). The identification of calmodulin (Melom and Littleton, 2013) and CN as suppressors of glial-originated seizures in *zyd* mutants indicates a Cam/CN-dependent pathway is hyperactivated and impairs normal cortex glial-to-neuronal soma signaling. Although the mechanism by which CN activity is upregulated in *Drosophila* cortex glia is different from that observed in mammals, the ability of CN to alter neuronal activity appears similar to mechanisms employed in glial-dependent neuroinflammatory states. During injury or disease states in mammals, activated astrocytes exhibit  $\text{Ca}^{2+}$  dysregulation with higher intracellular  $\text{Ca}^{2+}$  levels, more frequent  $\text{Ca}^{2+}$  oscillations and an elevated expression of  $\text{Ca}^{2+}$  channels and  $\text{Ca}^{2+}$ -regulated proteins (Kuchibhotla et al., 2009; Lin et al., 2007; Sama and Norris, 2013). While its clear how these changes would hyperactivate CN signaling, which has extreme consequences for neuronal function, it is unclear what role basal CN activity has in glial signaling. CN regulates the expression of several key  $\text{Ca}^{2+}$  mediators in multiple cell types (Carafoli et al., 1999; Genazzani et al., 1999; Graef et al., 1999; Groth et al., 2007), including plasma membrane  $\text{Ca}^{2+}$  channels, intracellular  $\text{Ca}^{2+}$  release channels, and  $\text{Ca}^{2+}$ -dependent enzymes (Baumgartel and Mansuy, 2012). However, no obvious phenotypes were observed when we decreased CN activity in *CanB2<sup>RNAi</sup>* cortex glia in control animals (Fig. 3C), suggesting the primary function of CN is only engaged following states of  $\text{Ca}^{2+}$  elevation in cortex glia during periods of strong neuronal activity.

The link between elevated glial  $\text{Ca}^{2+}$  signaling and defects in  $\text{K}^+$  buffering was an unexpected observation in the *zyd* mutant. Effective removal of  $\text{K}^+$  from the extracellular space is vital for maintaining brain homeostasis and limits network hyperexcitability during normal brain function, as disruptions in  $\text{K}^+$  clearance have been linked to several pathological conditions (David et al., 2009; Leis et al., 2005; Somjen, 2002). In addition to ion homeostasis, astrocytic  $\text{K}^+$  buffering has been suggested as a mechanism for promoting hyperexcitability and engaging specific network activity (Bellot-Saez et al., 2017; Wang et al., 2012a). Two mechanisms for

astrocytic  $K^+$  clearance have been previously identified, including net  $K^+$  uptake (mediated by the  $Na^+/K^+$  ATPase pump) and  $K^+$  spatial buffering (via passive  $K^+$  influx) (Bellot-Saez et al., 2017). However, the complete repertoire of  $K^+$  channels involved in spatial  $K^+$  buffering remains elusive (Ma et al., 2014). We found that cortex glial knockdown of the *Drosophila* KCN18/TRESK  $K_{2P}$  homolog sand triggered stress-induced seizures, indicating sand is involved in  $K^+$  homeostasis in the brain. Several studies have linked other members of the  $K_{2P}$  family, mainly TREK-1 and TWIK-1, to distinct aspects of astrocytic function. TREK-1 regulates fast glutamate release by astrocytes (Woo et al., 2012), TWIK-1 and TREK-1 mediate passive  $K^+$  conductance in astrocytes (Hwang et al., 2014), and TWIK-1 is recruited to the astrocytic membrane by mGluR3 activation (Wang et al., 2016).

We considered two potential mechanisms for CN regulation of sand, including direct dephosphorylation and altered endocytic trafficking. At rest, the mammalian sand homolog TRESK is constitutively phosphorylated. Following generation of a  $Ca^{2+}$  signal, TRESK is dephosphorylated and activated by CN (Enyedi and Czirjak, 2015). Constitutive dephosphorylation and activation of sand by CN could potentially result in higher  $K^+$  efflux from cortex glia and neuronal depolarization, leading to higher seizure susceptibility. However, in this scenario,  $K^+$  buffering upon hyperactivation of the nervous system should be more efficient, and thus less seizures are expected. Cortex glia knockdown of the two kinases that phosphorylate TRESK, PKA and Par-1, did not cause seizures. As such, we found no evidence that sand activity is regulated by CN dephosphorylation of the protein directly in cortex glia.

Beyond dephosphorylation, sand expression on the plasma membrane of specific sleep homeostat neurons in *Drosophila* is regulated by activity-induced internalization (Pimentel et al., 2016). Given astrocytes can shape neuronal circuit activity by actively altering their  $K^+$  uptake capabilities (Wang et al., 2012a), we propose that *Drosophila* cortex glia regulate the expression levels of sand (and potentially other  $K^+$  buffering proteins) on the cell membrane in a  $Ca^{2+}$ -regulated fashion in normal animals. When  $Ca^{2+}$  is constitutively elevated in *zgd* mutants, this regulation is thrown out of balance. Indeed, inhibition of endocytosis in cortex glia can rescue *zgd* seizures, suggesting that a membrane protein responsible for the neuronal hyperexcitability phenotype is being abnormally internalized in *zgd* cortex glia. Bypassing sand function by improving cortex glial  $K^+$  buffering/uptake capacity through overexpression of a leak  $K^+$  channel (EKO (White et al., 2001)) can reverse the *zgd* phenotype from seizures (caused by neuronal hyperactivity) to paralysis (caused by neuronal hypoactivity). Together, these findings indicate elevated  $Ca^{2+}$  levels lead to hyperactivation of CN and elevated endocytosis, sand internalization, and impairment in  $K^+$  buffering by cortex glia in *zgd* mutant animals (Fig. 7A).

Accumulating evidence indicate glia play contributive or even causative roles in several neurological disorders, neurodevelopmental syndromes and neurodegenerative diseases including epilepsy, Fragile X syndrome and SMA respectively. Increased glial activity is associated with abnormal neuronal excitability (Wetherington et al., 2008), and pathologic elevation of glial  $Ca^{2+}$  has been suggested to play an important role in the generation of seizures (Gomez-Gonzalo et al., 2010; Tian et al., 2005). Approximately 50 million people worldwide have epilepsy, making it one of the most common neurological diseases globally (World Health Organization, 2018, <http://www.who.int/en/>). The traditional view assumes that epileptogenesis occurs exclusively in neurons. However, an astrocytic basis for epilepsy was proposed almost two decades ago (Gomez-Gonzalo et al., 2010; Tashiro et al., 2002; Tian et al., 2005). In a non-pathological state, glia display  $Ca^{2+}$  oscillations spontaneously (Takata and Hirase, 2008) and in response to physiological neuronal activity (Wang et al., 2006). One widely-studied output of  $Ca^{2+}$  oscillations is gliotransmission, the glial release of certain transmitters (Agulhon et al., 2008; Lee et al., 2010). Indeed,  $Ca^{2+}$ -dependent glutamate release from astrocytes causes synchronous currents in neighboring neurons (Angulo et al., 2004; Fellin et al., 2006; Fellin et al., 2004), and is capable of eliciting action potentials (Pirttimaki et al., 2011), suggesting abnormally elevated glial  $Ca^{2+}$  may produce neuronal hypersynchrony through enhanced gliotransmission. In addition,

*in vivo* work demonstrated that several anti-epileptic drugs reduce glial  $\text{Ca}^{2+}$  oscillations (Tian et al., 2005). Although increased glial activity has been associated with abnormal neuronal excitability, the role of glia in the development and maintenance of seizures, and the exact pathway(s) by which abnormal glial  $\text{Ca}^{2+}$  alter glia-to-neuron communication and neuronal excitability are poorly characterized (Wetherington et al., 2008). A second proposed mechanism by which astrocytes regulate neuronal excitability and seizure susceptibility involves the uptake and redistribution of  $\text{K}^+$  ions (Bellot-Saez et al., 2017; Wang et al., 2012a) and neurotransmitters (Rose et al., 2017) from the extracellular space. In this study, we explored the pathways that are activated within glial cells in response to abnormally elevated glial  $\text{Ca}^{2+}$  that triggers seizures. We found that both mechanisms are at play in *Drosophila* cortex glial cells, with elevated intracellular  $\text{Ca}^{2+}$  leading to impaired  $\text{K}^+$  buffering. We identified several other suppressors of seizure induction in *zgd* mutants that are involved in GPCR signaling and vesicle trafficking, suggesting additional glial pathways may impact neuronal activity as well.

Current estimates suggest ~70% of children and adults with epilepsy can be successfully treated with current anti-epileptic drugs (World Health Organization, 2018, <http://www.who.int/en/>). The observation that several anti-epileptic drugs reduce glial  $\text{Ca}^{2+}$  oscillations *in vivo* (Tian et al., 2005), together with the fact that ~30% of epilepsy patients are non-responders, suggest that pharmacologically targeting glial pathways might be a promising avenue for future drug development in the field. Several neuronal seizure mutants in *Drosophila* have already been demonstrated to respond to common human anti-epileptic drugs, indicating key mechanisms that regulate neuronal excitability are conserved from *Drosophila* to humans. Indeed, *zgd*-induced seizures can be rescued when animals are fed a CN inhibitor (Fig. 4), indicating pharmacological targeting of the glial CN pathway can improve the outcome of a glial-derived seizure mutant. Prior studies have also shown improvement following treatment with the CN inhibitor FK506 in a rodent kindling model (Moia et al., 1994; Moriwaki et al., 1996). These data suggest CN activity regulates epileptogenesis in both *Drosophila* and mammalian models. Further characterization of how glia detect, respond, and actively shape neuronal excitability is critical to our understanding of neuronal communication and future development of new treatments for neurological diseases like epilepsy.

## Methods

### *Drosophila* genetics and molecular biology

Flies were cultured on standard medium at 22°C unless otherwise noted. *zydeco* (*zyd*<sup>1</sup>, here designated as *zyd*) mutants were generated by ethane methyl sulfonate (EMS) mutagenesis and identified in a screen for temperature-sensitive (TS) behavioral phenotypes. The UAS/Gal4 and LexAop/LexA systems were used to drive transgenes in glia, including repo-gal4, a pan-glial driver; NP2222-gal4, a cortex-glial specific driver; GMR54H02-gal4, expressed in a smaller set of cortex glial cells; and alm-gal4, an astrocyte-like glial cell specific driver. The *UAS-dsRNAi* flies used in the study were obtained from the VDRC (Vienna, Austria) or the TRiP collection (Bloomington *Drosophila* Stock Center, Indiana University, Bloomington, IN, USA). All screened stocks are listed in supplementary material (Table S2). *UAS-myrGCaMP6s* was constructed by replacing GCaMP5 in the previously described myrGCaMP5 transgenic construct. Transgenic flies were obtained by standard germline injection (BestGene Inc.). For all experiments described, only male larva and adults were used. In RNAi experiments, the animals also had the UAS-dicer2 transgenic element on the X chromosome to enhance RNAi efficiency. For survival assays, embryos were collected in groups of ~50 and transferred to fresh vials (n=3). 3<sup>rd</sup> instar larvae and/or pupae were counted. Survival rate (SR) was calculated as:

$$SR = \frac{N_{live\ 3rd\ instar\ animals}}{N_{embryos}}$$

For conditional expression using Tub-gal80<sup>ts</sup> (Figs. 1A, 2E and 6B), animals of the designated genotype were reared at 22°C to adulthood with gal80 suppressing gal4-driven transgene expression (*zyd*<sup>RNAi</sup>, *CanB2*<sup>RNAi</sup> and *Rab5*<sup>DN</sup>, respectively). Flies were then transferred to a 31°C incubator to inactivate gal80 and allow gal4 expression or knockdown for the indicated period. For inhibiting transgene expression in cortex glia (Fig. 5A) GMR54H02-lexA was used to express gal80 from LexAop-gal80. For inhibiting transgene expression specifically in neurons (Fig. 2D) C55-gal80 was used.

Stocks used in this study:

		#	Stock #/
Drivers	Repo-gal4		
	NP2222-gal4		
	GMR5H02-gal4		BDSC 45784
	C155-gal4		
RNAi	Cam		BDSC 34609
	CanB2	#1	BDSC 27270
	CanB2	#2	VDRC 104370
	CanB2	#3	VDRC 28764
	CanB2	#4	BDSC 38971
	<i>Pp2B-14D</i>	#1	BDSC 25929
	<i>Pp2B-14D</i>	#2	BDSC 40872
	<i>CanA-14F</i>	#1	BDSC 38966
	<i>CanA-14F</i>	#2	VDRC 30105
	Stim		BDSC 27263
	cac		VDRC 104168
	sand		VDRC 47977



	Rab5		BDSC 34832
	zyd		VDRG 40987
Other	UAS-EKO		BDSC 40973
	CalexA		BDSC 66542
	;Tub-gal80 <sup>ts</sup> ;		BDSC 7019
	::Tub-gal80 <sup>ts</sup>		BDSC 7018
	UAS- Pp2B-14F <sup>H217Q</sup>		DGGR 109869

Transgenic lines generated for this study:

	UAS- myrGCaMP6s		
	LexAop- myrGCaMP6s		

For a complete list of all RNAi stocks used in this study, see Table S2.

### Behavioral analysis:

All experiments were performed using groups of ~10-20 males.

#### 1. Temperature-sensitive seizures/zyd modifier screen:

Adult males aged 1-2 days were transferred in groups of ~10-20 flies ( $n \geq 3$ , total # of flies tested in all assays was always  $> 40$ ) into preheated vials in a water bath held at the indicated temperature with a precision of 0.1°C. Seizures were defined as the condition in which the animal lies incapacitated on its back or side with legs and wings contracting vigorously. Paralysis was defined as the condition in which the animal fell to the bottom of the vial and exhibited no movement. For screening purposes, only flies that showed normal wildtype-like behavior (i.e. walking up and down on vials walls) during heat-shock were counted as successful rescue. To analyze behavior in a more detailed manner we characterized four behavioral phenotypes: wall climbing (flies are climbing on vials walls), bottom dwelling (flies are on the bottom of the vial, standing/ walking without seizures), partial seizures (flies are on the bottom of the vial, seizing most of the time) and complete seizures (flies are constantly lying on their side or back with legs twitching). For assaying seizures in larvae, 3<sup>rd</sup> instar males were gently washed with PBS and transferred to 1% agarose plates heated to 38°C using a temperature-controlled stage. Larval seizures were defined as continuous, unpatterned contraction of the body wall muscles that prevented normal crawling behavior. For determining seizure temperature threshold, groups of 10 animal were heat-shocked to the indicated temperature (either 37.5, 38, 38.5 or 39°C). Threshold was defined as the temperature in which  $> 50\%$  of the animal were seizing after 1 minute.

#### 2. Bang sensitivity:

Adult male flies in groups of ~10-20 males ( $n=3$ ) were assayed 1-2 days post-eclosion. Flies were transferred into empty vials and allowed to rest for 1–2 h. Vials were vortexed at maximum speed for 10 seconds, and the number of flies that were upright and mobile was counted at 10 seconds intervals.

3. Light avoidance:

These assays were performed using protocols described previously following minor modifications. Briefly, pools of ~20 3<sup>rd</sup> instar larvae (108–120 hours after egg laying) were allowed to move freely for 5 minutes on Petri dishes with settings for the phototaxis assay (Petri dish lids were divided into quadrants, and two of these were blackened to create dark environment). The number of larvae in light versus dark quadrants was then scored (n=4). Response indices (RI) were calculated as:

$$RI = \frac{N_{Dark}}{total}$$

4. Activity monitoring using the MB5 system:

Adult flies activity was assayed using the multi-beam system (MB5, TriKinetics) as previously described. Briefly, individual males aged 1-3 days were inserted into 5 mm×80 mm glass pyrex tubes. Activity was recorded following a 20-30 minutes acclimation period. Throughout each experiment, flies were housed in a temperature- and light-controlled incubator (25°C, ~40-60% humidity). Post-acquisition activity analysis was performed using Excel to calculate activity level across 1-minute time bins (each experimental run contained 8 control animals and 8 experimental animals, n≥3).

5. Gentle touch assay

3<sup>rd</sup> instar male larvae (108–120 hours after egg laying) were touched on the thoracic segments with a hair during forward locomotion. No response, a stop, head retraction and turn were grouped into type I responses, and initiation of at least one single full body retraction or multiple full body retractions were categorized as type II reversal responses. Results were grouped to 20 males per assay (n=3).

## Electrophysiology

Intracellular recordings of wandering 3<sup>rd</sup> instar male larvae were performed in HL3.1 saline (in mm: 70 NaCl, 5 KCl, 4 MgCl<sub>2</sub>, 0.2 CaCl<sub>2</sub>, 10 NaHCO<sub>3</sub>, 5 Trehalose, 115 sucrose, 5 HEPES-NaOH, pH 7.2) containing 1.5 mm Ca<sup>2+</sup> using an Axoclamp 2B amplifier (Molecular Devices) at muscle fiber 6/7 of segments A3-A5. For recording the output of the central pattern generator, the CNS and motor neurons were left intact. Temperature was controlled with a Peltier heating device and continually monitored with a microprobe thermometer. Giant fiber recordings were performed as previously described.

## *In vivo* Ca<sup>2+</sup> imaging

UAS-*myrGCaMP6s* was expressed in glia with using the drivers described above. 2<sup>nd</sup> instar male larvae were washed with PBS and placed on a glass slide with a small amount of Halocarbon oil #700 (LabScientific). Larvae were turned ventral side up and gently pressed with a coverslip and a small iron ring to inhibit movement. Images were acquired with a PerkinElmer Ultraview Vox spinning disk confocal microscope and a high-speed EM CCD camera at 8–12 Hz with a 40X 1.3 NA oil-immersion objective using Volocity Software. Single optical planes within the ventral cortex of the ventral nerve cord (VNC) were imaged in the dense cortical glial region immediately below the surface glial sheath. Average myrGCaMP6s signal in cortex glia was quantified in the central abdominal neuromeres of the VNC within a manually selected ROI excluding the midline glia. Ca<sup>2+</sup> oscillations were counted within the first minute of imaging at room temperature, and then normalized to the ROI area.

## Drug feeding

Cyclosporin-A (Sigma Aldrich), FK506 (InvivoGen) and CN585 (Millipore) were dissolved in DMSO to a final concentration of 20 mM. Fly feeding solution included 5% yeast and 5% sucrose in water. Adult males less than 1 day old were starved for 6 hours and then transferred to a vial containing a strip of Wattman paper soaked in feeding solution containing the designated concentration of CN inhibitor, or DMSO as control. Flies were behaviorally tested following 6, 12 or 24 hours of drug feeding.

## Immunostaining and Western Analysis

For immunostaining, dissected 3<sup>rd</sup> instar male larvae were fixed with cold 4% paraformaldehyde in HL3.1 buffer for 45 minutes. Antibodies were used at the following dilutions: mouse anti-repo (8D12 Developmental Studies Hybridoma Bank), 1:50; rat anti-ELAV (7E8A10, Developmental Studies Hybridoma Bank), 1:50; GFP Rabbit IgG, Alexa Fluor® 488 Conjugate (Thermo Fisher, 1:500); Goat anti mouse Alexa Fluor® 405 Conjugate (Life technologies, 1:2000) and Goat anti-rat Alexa Fluor® 555 Conjugate (Invitrogen, 1:2000). Larvae were mounted in VECTASHIELD (Vector Labs) and imaged on a Zeiss LSM800 confocal microscope with ZEN software (Carl Zeiss MicroImaging) with oil-immersion 63/1.4 NA objectives. Rab5::GFP puncta ( $>0.1 \mu\text{m}^2$ ) were detected automatically within a set circular ROI (with  $r=5 \mu\text{m}$ , centroid in the center of the repo positive nucleus) using Volocity software. Western blotting of adult whole-head and larval brain lysates was performed using standard laboratory procedure. Nitrocellulose membranes were probed with rabbit anti-cleaved DCP1 (Cell Signaling, 1:1000) and rabbit anti-GFP (Abcam, 1:500). Equal loading was assayed using mouse anti-syx1A (1:1000). Primaries were detected with Alexa Fluor 680-conjugated and 800-conjugated anti-rabbit and anti-mouse (Invitrogen, 1:3000). Western blots were visualized with an Odyssey infrared scanner (Li-Cor).

## Statistical analysis

No statistical methods were used to predetermine sample size. All  $n$  numbers represent biological replicates. Data were pooled from 2–3 independent experiments. Immunofluorescence experiments ( $\text{Ca}^{2+}$  imaging, CalexA expression and Rab5 puncta characterization) were randomized and blinded. P values are represented as  $*=P<0.05$ ,  $**=P<0.01$ ,  $***=P<0.001$ ,  $****=P<0.0001$ .  $P < 0.05$  was considered significant. All data are expressed as mean  $\pm$  SEM.

## Acknowledgements

This work was supported by NIH grants NS40296 and MH104536 to J.T.L. We thank the Bloomington *Drosophila* Stock Center (NIH P40OD018537), the Vienna *Drosophila* RNAi Center, the Harvard TriP Project, the KYOTO Stock Center, Marc Freeman (Vollum Institute) and Gerald Rubin (Janelia Research Campus) for providing *Drosophila* strains, the Developmental Studies Hybridoma Bank for antisera, Mark Tanouye for help with GF recordings, and members of the Littleton lab for helpful discussions and comments on the manuscript.

## Author Contributions

S.W. performed the *zydeco* genetic interaction screen, confocal imaging, biochemistry, and behavioral analysis. J.E.M. assisted with the genetic modifier screen. K.G.O. and Y.V.Z.

performed the electrophysiology. J.T.L supervised the project. S.W. and J.T.L. designed experiments and wrote the paper.

### **Declaration of Interests**

The authors declare no competing interests.

## Figures:

Figure 1

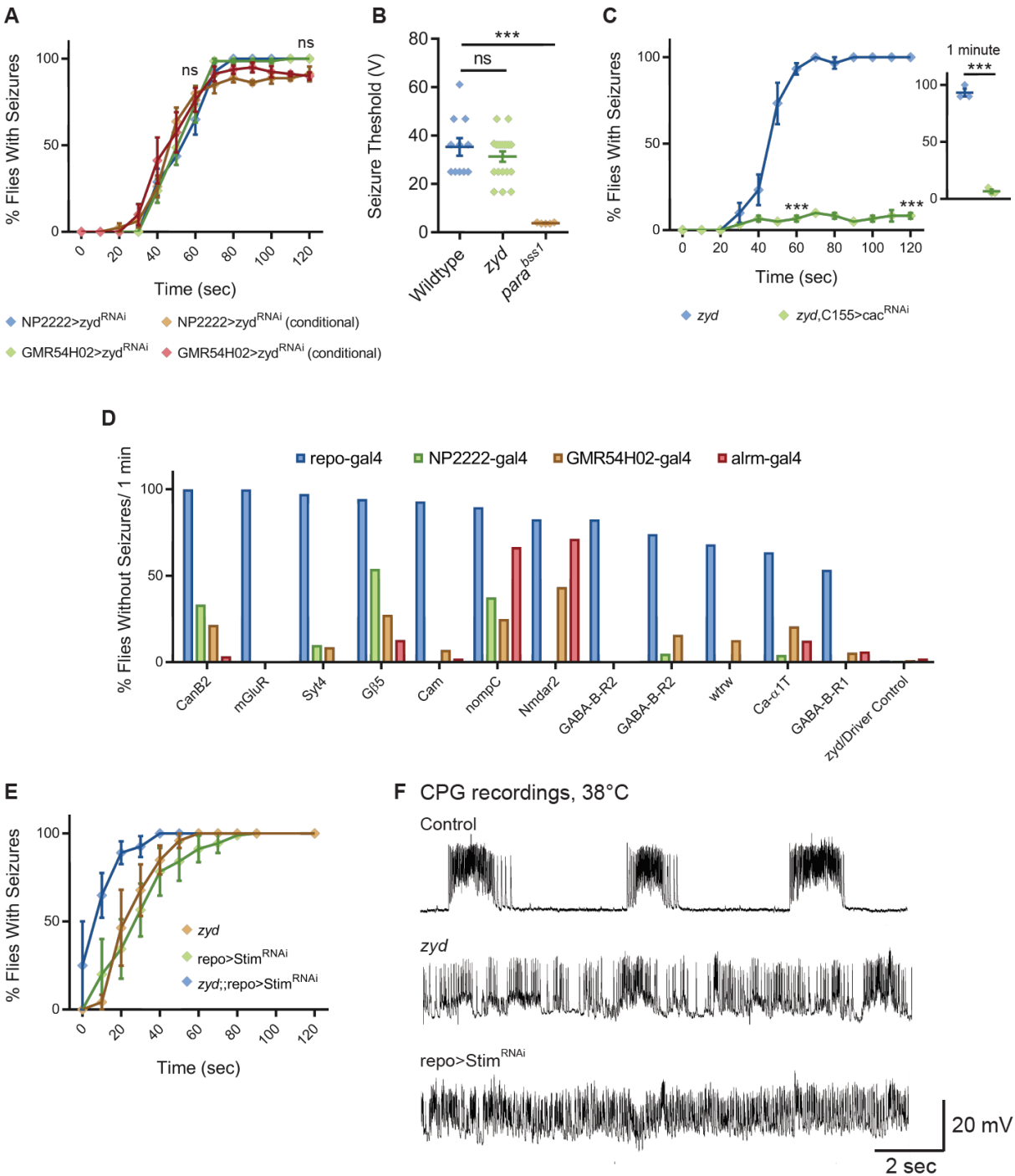


**Figure 1. Mutations in a cortex glial NCKX generate stress-induced seizures.**

**A.** Time course of heat-shock-induced seizures (38.5°C, HS) following chronic or conditional knockdown of *zyd* with two different cortex glial drivers (NP2222 and GMR54H02) is shown. Rearing adult flies in the restrictive temperature (>30°C) for *gal80<sup>ts</sup>* (a temperature-sensitive form of the *gal4* inhibitor, *gal80*, see methods) relieves *gal80* inhibition of *gal4* and allows expression of *zyd<sup>RNAi</sup>* only in adult stage. These manipulations reproduce the *zyd* mutant seizure phenotype (N=4 groups of 20 flies/ genotype). **B.** Giant fiber recordings of seizure threshold in wildtype, *zyd* and *Para<sup>bss1</sup>* (as positive control) are shown. The voltage required to induce seizures in *zyd* is not significantly different from wildtype (35.32 ± 3.65V and 31.33 ± 2.12V, p=0.3191, n≥7 flies/genotype). **C.** Behavioral analysis of the time course of HS-induced seizures indicates neuronal knockdown of *cac* (*C155>cac<sup>RNAi</sup>*) rescues the *zyd* seizure phenotype. Inset shows results after 1 minute of HS (p=0.0004, N=4 groups of 20 flies/genotype). **D.** Histogram summarizing seizure suppression of top hits obtained from an interaction screen for the *zyd* TS seizure phenotype (also see supplemental table S1). Four *gal4* drivers were used: *repo-gal4* (pan-glial); NP2222-*gal4* (cortex glia); GMR54H02 (cortex glia) and *alm-gal4* (astrocyte glia). (n≥30 flies/2 independent crosses/RNAi tested). **E.** Behavioral analysis of the time course of HS-induced seizures shows that pan-glial knockdown of *Stim* on a wildtype background leads to seizures with similar kinetics to those observed in *zyd* mutants. Pan-glial knockdown of *Stim* in *zyd* mutants decreases the time to seizure onset (N=4 groups of ≥15 flies/ genotype). **F.** Representative voltage traces of spontaneous central pattern generator (CPG) motor activity at larval 3<sup>rd</sup> instar muscle 6 at 38°C in wildtype, *zyd* and *repo>Stim<sup>RNAi</sup>* (n≥5 preparations/genotype). Error bars are SEM, \*\*\*=P<0.001, Student's t-test.

Figure 2

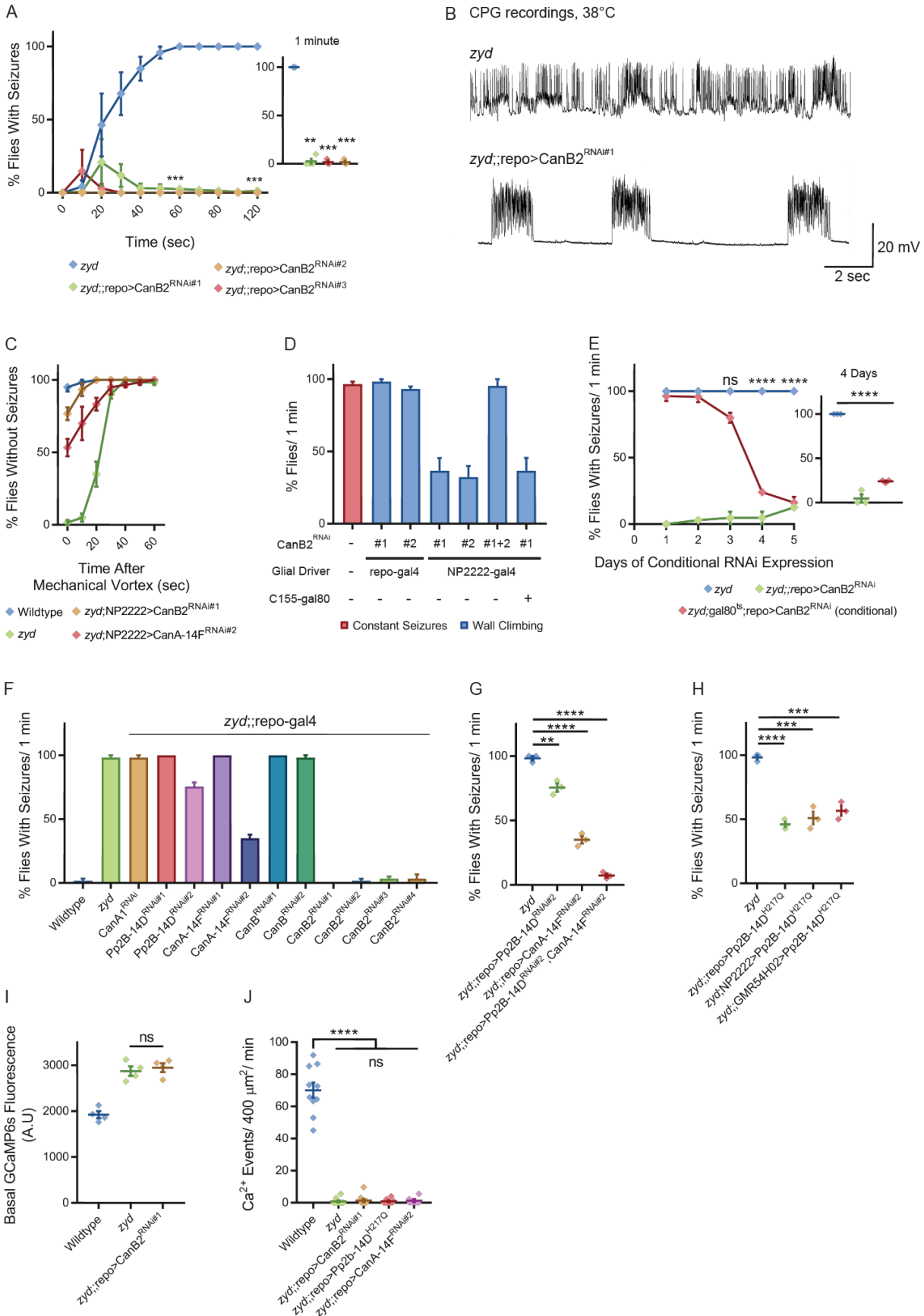


**Figure 2. Cortex glial knockdown of calcineurin rescues *zyd* seizures without affecting intracellular Ca<sup>2+</sup>.**

**A.** Behavioral analysis of HS-induced seizures. Pan-glial knockdown of the CN regulatory subunit, CanB2, with three different hairpins (#1, #2 and #3, see methods) rescues the *zyd* seizure phenotype (N=4 groups of ≥15 flies/genotype). Inset shows analysis after 1 minute of HS (p=0.0001). **B.** Representative voltage traces of spontaneous CPG activity at larval 3<sup>rd</sup> instar muscle 6 at 38°C in *zyd* and *zyd*;repo>CanB2<sup>RNAi#1</sup> animals (n≥5 preparations/genotype). **C.** Behavioral analysis of the recovery from vortex-induced seizures. Pan-glial knockdown of CanB2 and CanA-14F rescues *zyd* vortex-induced seizures (N=3 groups of 20 flies/genotype). **D.** Detailed analysis (see methods) of HS induced behaviors of *zyd*/CanB2<sup>RNAi</sup> flies. Cortex glial knockdown of CanB2 leads to seizure rescue in ~30% of *zyd*;NP2222>CanB2<sup>RNAi</sup> flies, with the remaining ~70% displaying partial rescue. Cortex glial CanB2 knockdown with two copies of the RNAi (*zyd*;NP2222>CanB2<sup>2xRNAi</sup>) recapitulates the full rescue seen with pan-glial knockdown. Inhibiting gal4 expression of the RNAi in neurons with gal80 (C155-gal80) does not alter the rescue observed with cortex glial knockdown (N=3 groups of >15 flies/genotype, see supplemental Fig. S2B for complete dataset). **E.** Cortex glial conditional knockdown of CanB2 using gal4/gal80<sup>ts</sup>. Rearing adult flies in the restrictive temperature (>30°C) for gal80<sup>ts</sup> (a temperature-sensitive form of the gal4 inhibitor, gal80) relieves gal80 inhibition of gal4 and allows expression of CanB2<sup>RNAi</sup> only in adult stage. A significant reduction in seizures (p<0.0001) was seen after four days of rearing flies at the restrictive temperature for gal80<sup>ts</sup> (31°C), with only ~25% of adults showing seizures. The reduction in seizures was enhanced when adults were incubated at 31°C for longer periods (N=3 groups of >10 flies/genotype). Inset shows analysis after 4 days of incubation at 31°C (p=0.0001). **F.** Pan-glial knockdown of the *Drosophila* calcineurin (CN) family (CanA1, CanA-14D/ Pp2B-14D, CanA-14F, CanB and CanB2) indicate CanB2 knockdown completely rescues *zyd* seizures, CanA14D and CanA14F knockdowns partially reduce seizures, and knockdown of either CanA1 or CanB do not alter the *zyd* phenotype (N=4 groups of >10 flies/genotype). **G.** Pan-glial knockdown of CanA14D and CanA14F partially rescues the *zyd* HS seizures phenotype (~25% rescue for CanA14D, p=0.0032; and ~60% rescue for CanA14F, p<0.0001). Knocking down the two genes simultaneously rescues *zyd* seizures, with only ~10% of flies showing seizures (~90% rescue, p<0.0001, N=3 groups of >10 flies/genotype). **H.** Overexpressing a dominant-negative form on Pp2B-14D (CanA<sup>H217Q</sup>) rescues ~50% of *zyd* seizures regardless of the driver used (repo: p<0.0001; NP2222: p=0.0006; GMR54H02-p=0.0004. N=3 groups of >10 flies/ genotype). **I.** Larval Ca<sup>2+</sup> imaging in cortex glia expressing myrGCaMP6s indicates the elevated basal Ca<sup>2+</sup> fluorescence at 25°C observed in *zyd* mutants



relative to wildtype cortex glia ( $p=0.0003$ ) is not altered following CanB2 knockdown (*zyd*; ;repo>CanB2<sup>RNAi</sup>,  $p=0.6096$ .  $n \geq 5$  animals/genotype). **J.** Microdomain  $Ca^{2+}$  oscillations observed in wildtype cortex glia expressing myrGCaMP6s are abolished in *zyd* cortex glia and are not restored following either CanB2 or CanA14F knockdown ( $n \geq 5$  animals/genotype). Error bars are SEM, \*\*= $P < 0.01$ , \*\*\*= $P < 0.001$ , \*\*\*\*= $P < 0.0001$ , Student's t-test.

Figure 3

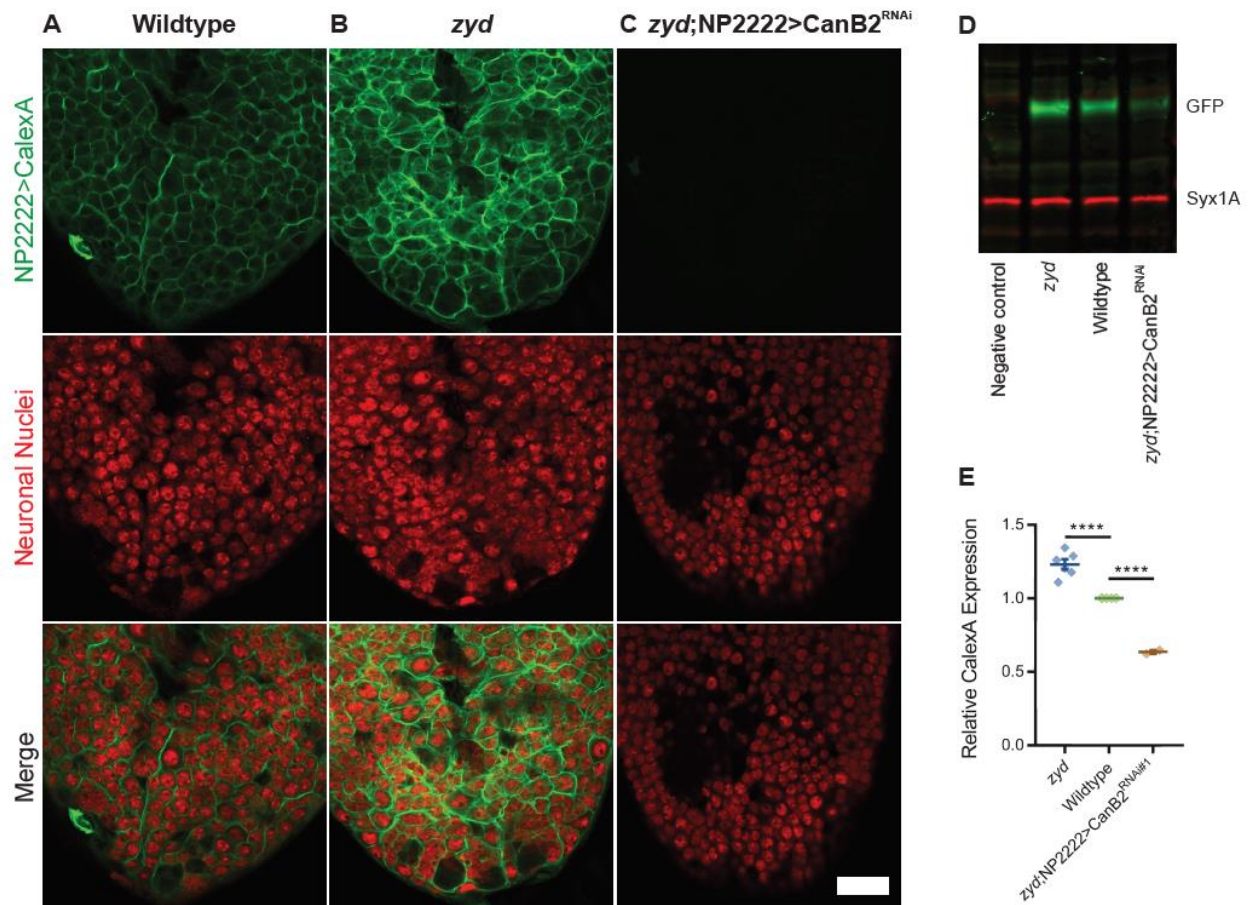


**Figure 3. Calcineurin activity is enhanced in *zyd* cortex glia and can be efficiently suppressed by CanB2 knockdown.**

**A-C.** Fluorescence microscopy imaging of cortex glial CalnexA-derived GFP expression in wildtype (A), *zyd* (B) and *zyd*;NP2222>CanB2<sup>RNAi</sup> (C) larvae. Red: anti-elav=neuronal nuclei; green: anti-GFP=cortex glial CN activity (animals were reared at 25°C, Scalebar = 20  $\mu$ m, N $\geq$ 5 animals/genotype). **D-E.** Western blot analysis of cortex glial CalnexA derived (NP2222>CalnexA) GFP expression in *zyd*, wildtype and *zyd*;NP2222>CanB2<sup>RNAi</sup> adult heads. CN activity is enhanced by ~25% (p<0.0001) in *zyd* cortex glia and reduced by ~35% (p<0.0001) in CanB2<sup>RNAi</sup> animals (N $\geq$ 2 experiment, 5 heads/sample). GFP signals in each experiment were normalized to wildtype. Error bars are SEM, \*\*\*\*=P<0.0001, Student's t-test.

Figure 4

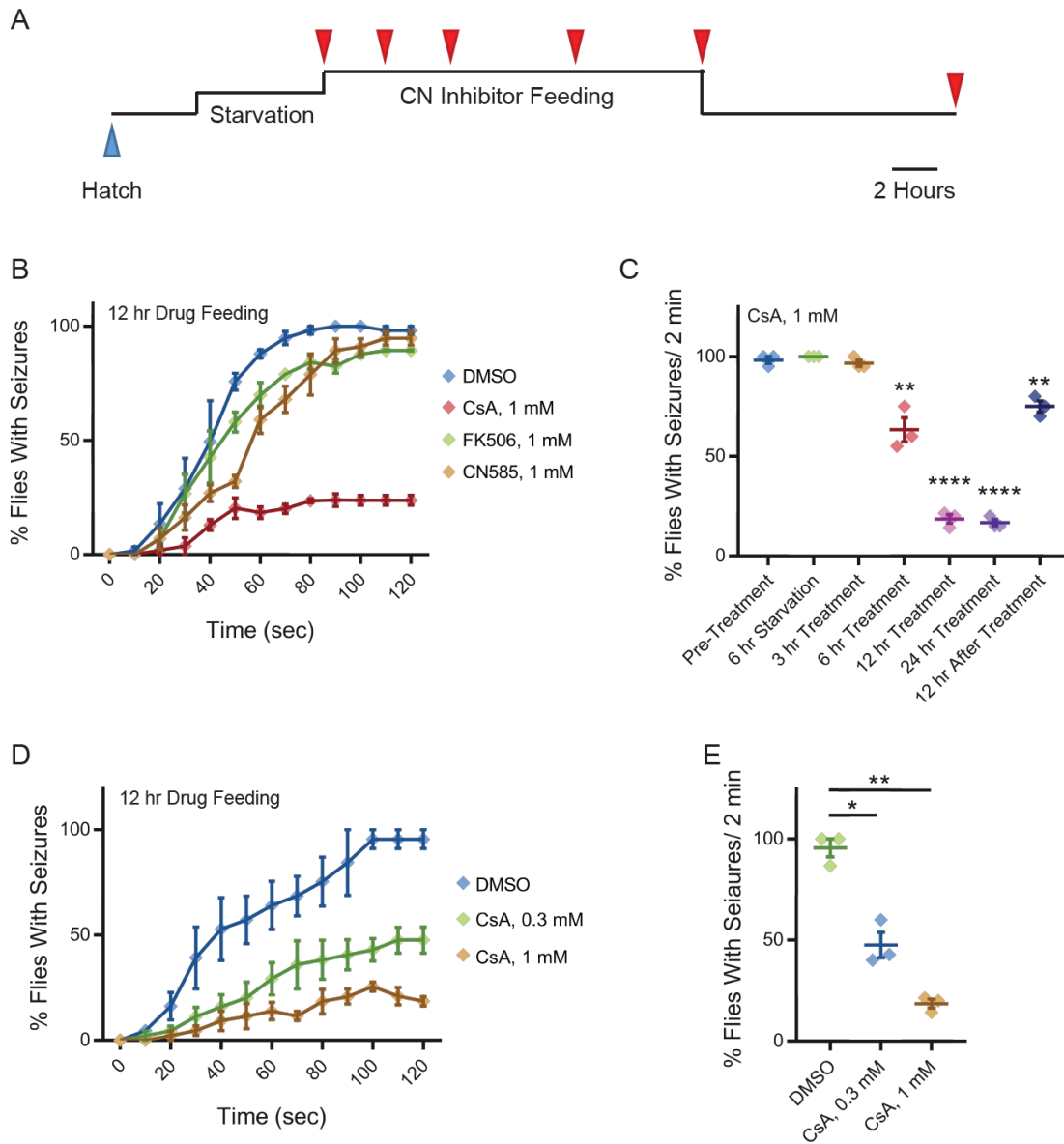


**Figure 4. Pharmacologically targeting calcineurin activity suppresses *zyd* heat-shocked induced seizures.**

**A.** Schematic representation of the experimental design. Adult male flies (<1 day old) were starved for 6 hours and fed with liquid medium containing CN inhibitors for 3, 6, 12 or 24 hours (red arrowheads), before testing for HS induced seizures. Flies were also tested 12 and 24 hours after drug withdrawal. **B-E.** Behavioral analysis of HS induced seizures. **B.** Flies were fed with 1 mM of either CsA, FK506 or CN585 for 12 hours. Feeding with 1 mM CsA reduces seizures by

~75% ( $p < 0.0001$ ), while the other two treatments had no significant effect. **C.** Summary of all time points for CsA treatment (N=3 groups of 15-20 flies/treatment. 6 hours feeding:  $p = 0.005$ ; 12/24 hours feeding:  $p < 0.0001$ ; 12 hours drug withdrawal:  $p = 0.0022$ ). **D-E.** The effect of CsA treatment on HS-induced seizures shows a significant dose-dependent reduction in seizure occurrence (N=3 groups of >15 flies/treatment). **E.** After 2 minutes of heat-shock, seizures were reduced by ~50% ( $p = 0.041$ ) in flies that were fed with 0.3 mM CsA, and by ~80% ( $p = 0.0062$ ) in flies that were fed with 1 mM CsA (N=3 groups of >15 flies/treatment). Error bars are SEM, \*= $P < 0.05$ , \*\*= $P < 0.01$ , \*\*\*\*= $P < 0.0001$ , Student's t-test.

Figure 5

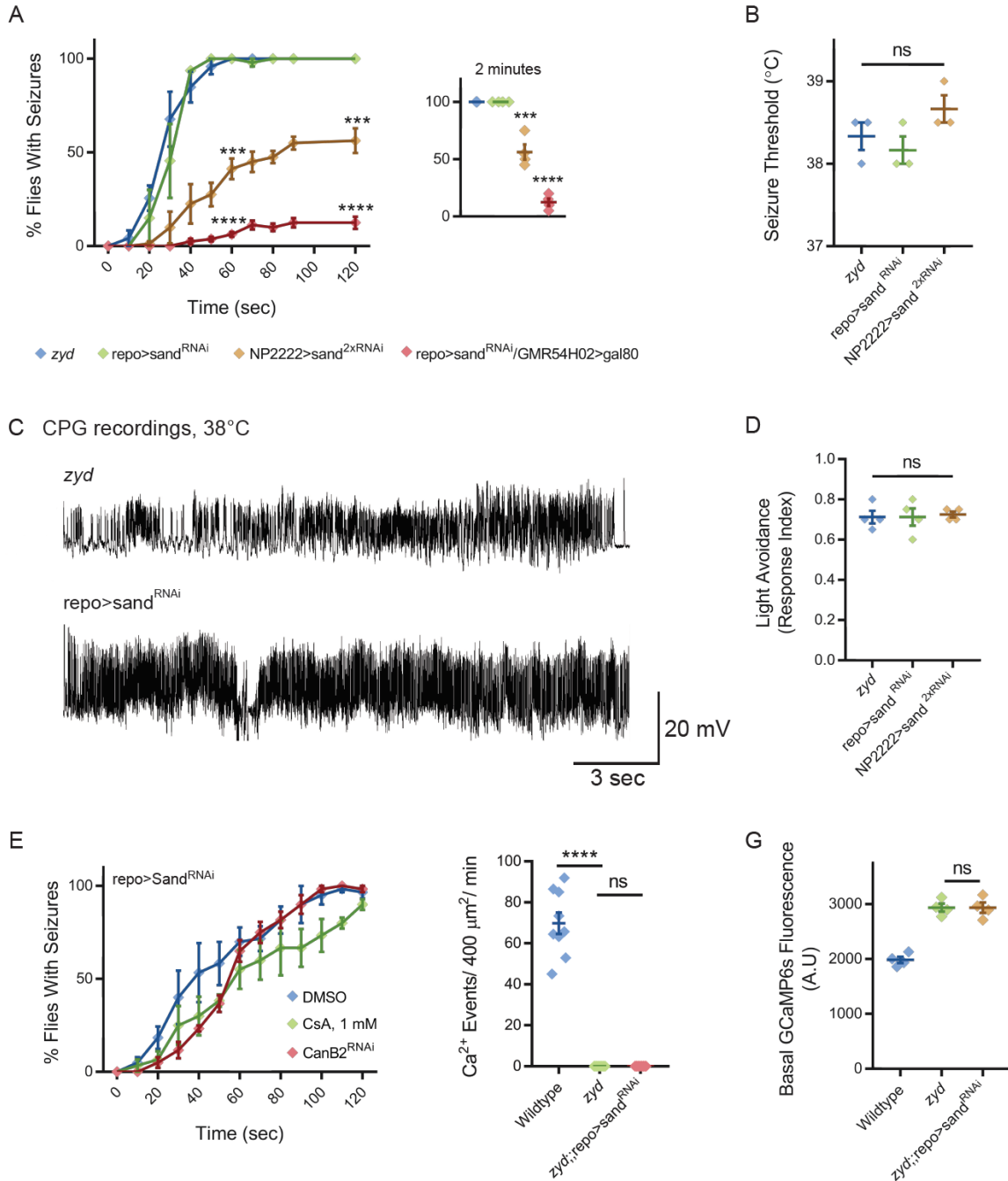


**Figure 5. Cortex glial knock-down of sandman, a  $K_{2P}$  channel, reproduces *zyd* phenotypes.**

**A-B.** Behavioral analysis of HS induced seizures. **A.** Knock down of sandman (sand) in different glial subtypes: pan-glial (repo), cortex glial (NP2222) and in all glia other than cortex glia (*repo>sand<sup>RNAi</sup>/GMR54H02>gal80* in which gal80 is constitutively inhibiting gal4 activity and

sand<sup>RNAi</sup> expression specifically in cortex glia). Inset shows analysis after 2 minutes of HS ( $p=0.0006$  for NP2222>sand<sup>2xRNAi</sup>,  $p<0.0001$  for repo>sand<sup>RNAi</sup>/GMR54H02-gal80, N=4 groups of >10 flies/genotype). **B.** Temperature threshold of repo-sand<sup>RNAi</sup> ( $p=0.5185$ ) and NP2222>sand<sup>2xRNAi</sup> ( $p=0.2302$ ) seizures in comparison to *zyd* (N=3 groups of 10/temperature/genotype). **C.** Representative voltage traces of spontaneous CPG activity at larval 3<sup>rd</sup> instar muscle 6 at 38°C in *zyd* and repo>sand<sup>RNAi</sup> ( $n\geq 5$  preparations/genotype). **D.** Light avoidance assay reveals no defect in this behavior at 25°C (N=3 groups of 20 flies/genotype). **E.** Behavioral analysis of HS-induced seizures. Seizures in repo>sand<sup>RNAi</sup> animals were not suppressed with either CanB2<sup>RNAi#1</sup> or by feeding flies with 1 mM (N=3 groups of 20 flies/treatment). **F-G.** Ca<sup>2+</sup> imaging in larval cortex glial cells using myrGCaMP6s. **F.** The average rate of microdomain Ca<sup>2+</sup> events was reduced in repo>sand<sup>RNAi</sup> cortex glia relative to wildtype ( $20.36 \pm 5.5$  and  $69.83 \pm 5.3$ ,  $p<0.0001$ ). Knockdown of sand on the *zyd* background did not restore *zyd* Ca<sup>2+</sup> microdomain events ( $n\geq 5$  animals/genotype). **G.** Average myrGCaMP6s fluorescence in cortex glia at 25°C. Elevated basal fluorescence of GCaMP6s in *zyd* relative to wildtype cortex glia ( $p=0.0003$ ) is not altered following sand knockdown (*zyd*;repo>sand<sup>RNAi</sup>, N=4 animals/genotype). Error bars are SEM, \*= $P<0.05$ , \*\*= $P<0.01$ , \*\*\*= $P<0.001$ , \*\*\*\*= $P<0.0001$ , Student's t-test.

**Figure 6**

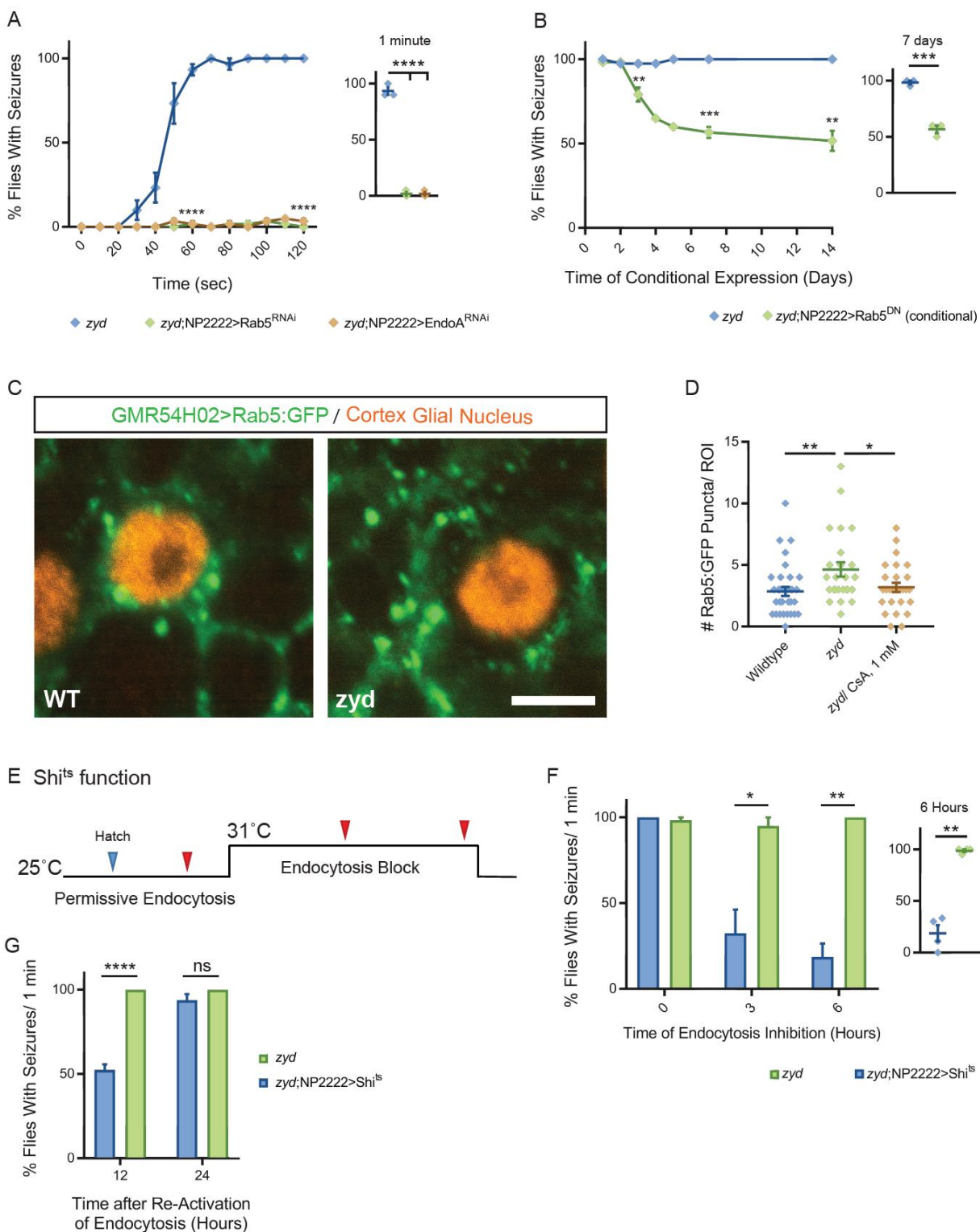


**Figure 6. Cortex glial inhibition of endocytosis rescues *zyd* seizures.**

**A-B.** Behavioral analysis of HS induced seizures. **A.** Cortex glial knockdown of Rab5 and EndoA rescues seizures in the *zyd* mutant. Inset shows effects at 1 minute of HS (N=3 groups of 20 flies/genotype,  $p < 0.0001$  at 1 minute and 2 minutes). **B.** Cortex glial conditional overexpression of dominant-negative Rab5 (Rab5<sup>DN</sup>) using UAS/gal4/gal80<sup>ts</sup>. Rearing adult flies in the restrictive temperature ( $>30^{\circ}\text{C}$ ) for gal80<sup>ts</sup> (a temperature-sensitive form of the gal4 inhibitor, gal80) relieves gal80 inhibition of gal4 and allows expression of Rab5<sup>DN</sup> only in adult stage. A significant reduction in seizures ( $p = 0.0044$ ) was seen after four days of incubation at the restrictive temperature for gal80<sup>ts</sup> ( $31^{\circ}\text{C}$ ), with ~60% flies showing seizures. The reduction in seizures was enhanced when flies were incubated at  $31^{\circ}\text{C}$  for longer periods (7 days:  $p = 0.0004$ , 14 days:  $p = 0.0083$ ). Inset shows analysis after 7 days of incubation at  $31^{\circ}\text{C}$  (N=3 groups of  $>10$  flies/genotype/time point). **C.** Fluorescence images showing accumulation of Rab5::GFP puncta in *zyd* cortex glia relative to wildtype cortex glia. Rab5::GFP was expressed using a cortex glial-specific driver (GMR54H02-gal4. Scale bar=5  $\mu\text{m}$ .  $n \geq 5$  animals/genotype). **D.** Analysis of the number of large ( $>0.1 \mu\text{m}^2$ ) Rab5::GFP puncta in wildtype and *zyd* cortex glia. The number of Rab5::GFP puncta in *zyd* cortex glia was increased relative to wildtype (average of  $4.64 \pm 0.58$  and  $2.85 \pm 0.37$  puncta/ROI respectively,  $p = 0.0088$ ). The number of large Rab5::GFP puncta in *zyd* treated with 1 mM CsA for 24 hours was decreased relative to *zyd* (average of  $3.19 \pm 0.37$  puncta/ROI,  $p = 0.0378$ .  $n \geq 25$  ROIs/3 animals/genotype/treatment). **E-F.** Conditional inhibition of endocytosis by cortex glial overexpression of shi<sup>ts</sup>. **E.** Schematic representation of the experimental design. Adult *zyd*; NP2222>shi<sup>ts</sup> male flies ( $>1$  day old) were incubated at the shi<sup>ts</sup> restrictive temperature ( $31^{\circ}\text{C}$ ) for 3 or 6 hours and then tested for HS-induced seizures (red arrowheads, N=3 groups of  $>15$  flies/time point). **F-G.** Behavioral analysis of HS induced seizures. **F.** A significant reduction in seizures is observed in flies that were incubated at  $31^{\circ}\text{C}$  for 3 hours ( $p = 0.0283$ ) or 6 hours ( $p = 0.013$ ). Inset shows analysis after 6 hours of incubation at  $31^{\circ}\text{C}$  (N=3 groups of  $>15$  flies/time point). **G.** *zyd*;NP2222>Shi<sup>ts</sup> flies seizures re-occur after removal from the Shi<sup>ts</sup> restrictive temperature (N=4 groups of 10-15 animals/time point; 12 hours:  $p < 0.0001$ ). Error bars are SEM, \*= $P < 0.05$ , \*\*= $P < 0.01$ , \*\*\*= $P < 0.001$ , \*\*\*\*= $P < 0.0001$ , Student's t-test.



Figure 7

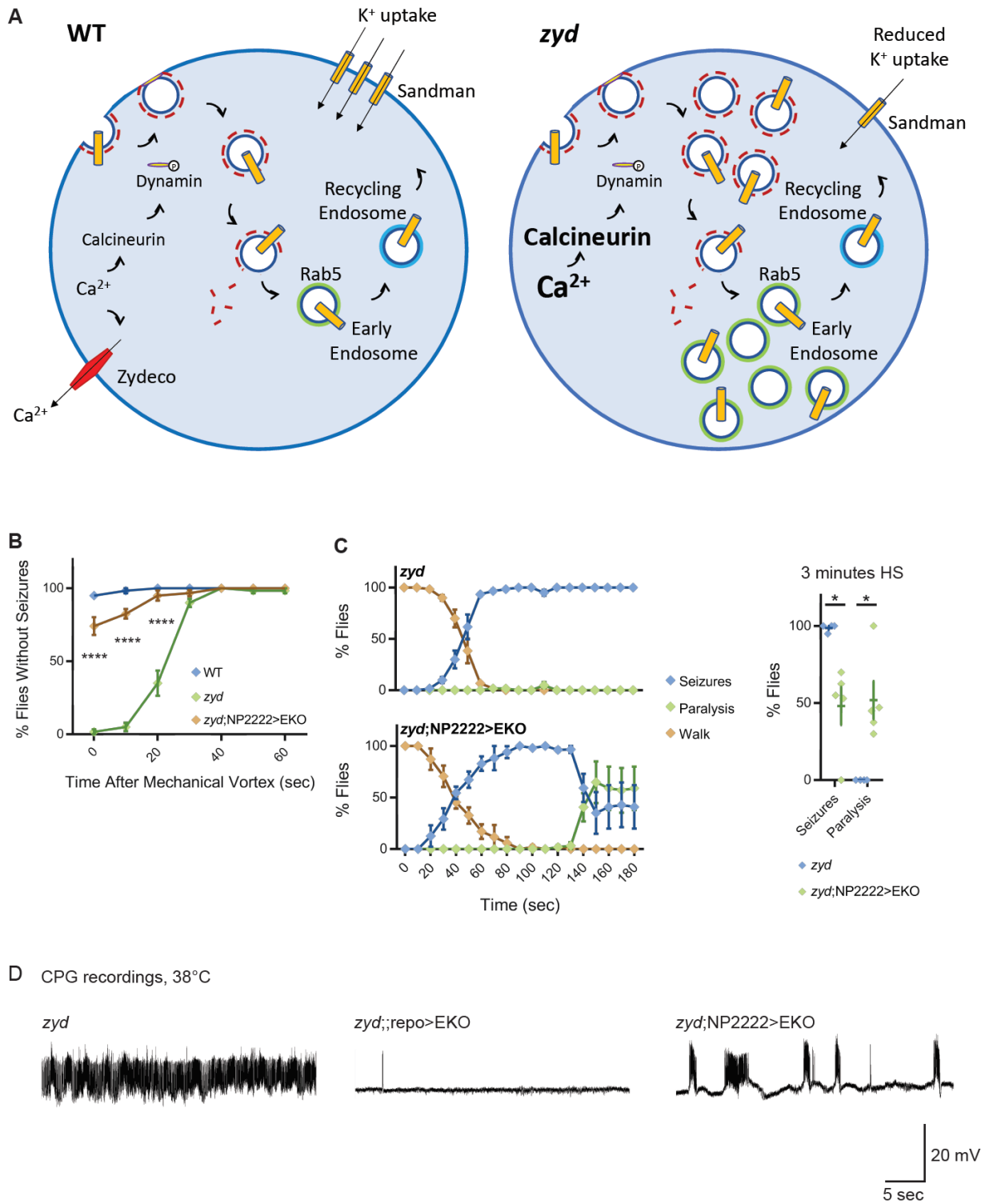


Figure 7: Enhancing glial  $K^+$  buffering by overexpressing a leak  $K^+$  channel rescues *zyd* seizures.

**A.** The current model for *zyd* function in seizure susceptibility is depicted. In wildtype (WT) cortex glia (left), oscillatory  $\text{Ca}^{2+}$  signaling maintains normal cortex glia-to-neuron communication and a balanced extracellular ionic environment. In *zyd* cortex glia (right), the basal elevation of  $\text{Ca}^{2+}$  leads to hyperactivation of CN and enhanced endocytosis with accumulation of early endosomes. This disrupts the endo-exocytosis balance of cortex glial membrane proteins such as  $\text{K}_{2\text{P}}$  leak channel sandman that regulate neuronal excitability. Knockdown of sandman mimics the *zyd* phenotype and the protein acts downstream of CN, indicating impaired extracellular  $\text{K}^{+}$  homeostasis causes neuronal hyperexcitability and hyperactivity in *zyd* mutants. **B-D.** Overexpression of a genetically modified constitutively-open Shaker  $\text{K}^{+}$  channel (termed EKO) modifies the *zyd* phenotype. **B.** *zyd* vortex-induced seizures are suppressed by ~80% in *zyd*; NP2222>EKO flies relative to *zyd* alone ( $p < 0.0001$ ,  $N = 3$  groups of 20 flies/genotype). **C.** During a HS, *zyd*; NP2222>EKO flies transition from early seizures to hypoactivity and paralysis. Inset shows analysis after 3 minutes of HS (seizures:  $p = 0.009$ ; paralysis:  $p = 0.008$ ,  $N = 5$  groups of 20 flies/genotype). **D.** Representative voltage traces of spontaneous CPG activity at 3<sup>rd</sup> instar larval muscle 6 at 38°C in *zyd*, *zyd*;repo>EKO and *zyd*;NP2222>EKO ( $n \geq 3$  preparations/genotype). EKO expression in all glia or only cortex glia eliminates the continuous CPG seizures observed in *zyd* mutants. Error bars are SEM, \*= $P < 0.05$ , \*\*\*\*= $P < 0.0001$ , Student's t-test.

## References

Abdul, H.M., Furman, J.L., Sama, M.A., Mathis, D.M., and Norris, C.M. (2010). NFATs and Alzheimer's Disease. *Mol Cell Pharmacol* 2, 7-14.

Agulhon, C., Fiacco, T.A., and McCarthy, K.D. (2010). Hippocampal short- and long-term plasticity are not modulated by astrocyte Ca<sup>2+</sup> signaling. *Science* 327, 1250-1254.

Agulhon, C., Petravicz, J., McMullen, A.B., Sweger, E.J., Minton, S.K., Taves, S.R., Casper, K.B., Fiacco, T.A., and McCarthy, K.D. (2008). What is the role of astrocyte calcium in neurophysiology? *Neuron* 59, 932-946.

Akagawa, H., Hara, Y., Togane, Y., Iwabuchi, K., Hiraoka, T., and Tsujimura, H. (2015). The role of the effector caspases drICE and dcp-1 for cell death and corpse clearance in the developing optic lobe in *Drosophila*. *Dev Biol* 404, 61-75.

Allen, N.J., and Barres, B.A. (2009). Neuroscience: Glia - more than just brain glue. *Nature* 457, 675-677.

Altenhein, B., Becker, A., Busold, C., Beckmann, B., Hoheisel, J.D., and Technau, G.M. (2006). Expression profiling of glial genes during *Drosophila* embryogenesis. *Dev Biol* 296, 545-560.

Angulo, M.C., Kozlov, A.S., Charpak, S., and Audinat, E. (2004). Glutamate released from glial cells synchronizes neuronal activity in the hippocampus. *J Neurosci* 24, 6920-6927.

Awasaki, T., Lai, S.L., Ito, K., and Lee, T. (2008). Organization and postembryonic development of glial cells in the adult central brain of *Drosophila*. *J Neurosci* 28, 13742-13753.

Azevedo, F.A., Carvalho, L.R., Grinberg, L.T., Farfel, J.M., Ferretti, R.E., Leite, R.E., Jacob Filho, W., Lent, R., and Herculano-Houzel, S. (2009). Equal numbers of neuronal and nonneuronal cells make the human brain an isometrically scaled-up primate brain. *J Comp Neurol* 513, 532-541.

Baalman, K., Marin, M.A., Ho, T.S., Godoy, M., Cherian, L., Robertson, C., and Rasband, M.N. (2015). Axon initial segment-associated microglia. *J Neurosci* 35, 2283-2292.

Battefeld, A., Klooster, J., and Kole, M.H. (2016). Myelinating satellite oligodendrocytes are integrated in a glial syncytium constraining neuronal high-frequency activity. *Nat Commun* 7, 11298.

Baumgartel, K., and Mansuy, I.M. (2012). Neural functions of calcineurin in synaptic plasticity and memory. *Learn Mem* 19, 375-384.

Bellot-Saez, A., Kekesi, O., Morley, J.W., and Buskila, Y. (2017). Astrocytic modulation of neuronal excitability through K(+) spatial buffering. *Neurosci Biobehav Rev* 77, 87-97.

Bindocci, E., Savtchouk, I., Liaudet, N., Becker, D., Carriero, G., and Volterra, A. (2017). Three-dimensional Ca(2+) imaging advances understanding of astrocyte biology. *Science* 356.

Carafoli, E., Genazzani, A., and Guerini, D. (1999). Calcium controls the transcription of its own

transporters and channels in developing neurons. *Biochem Biophys Res Commun* 266, 624-632.

Chen, Y., Holstein, D.M., Aime, S., Bollo, M., and Lechleiter, J.D. (2016). Calcineurin beta protects brain after injury by activating the unfolded protein response. *Neurobiol Dis* 94, 139-156.

Cornell-Bell, A.H., Finkbeiner, S.M., Cooper, M.S., and Smith, S.J. (1990). Glutamate induces calcium waves in cultured astrocytes: long-range glial signaling. *Science* 247, 470-473.

Coutinho-Budd, J.C., Sheehan, A.E., and Freeman, M.R. (2017). The secreted neurotrophin Spatzle 3 promotes glial morphogenesis and supports neuronal survival and function. *Genes Dev* 31, 2023-2038.

Czirjak, G., Toth, Z.E., and Enyedi, P. (2004). The two-pore domain K<sup>+</sup> channel, TRESK, is activated by the cytoplasmic calcium signal through calcineurin. *J Biol Chem* 279, 18550-18558.

Dani, J.W., Chernjavsky, A., and Smith, S.J. (1992). Neuronal activity triggers calcium waves in hippocampal astrocyte networks. *Neuron* 8, 429-440.

David, Y., Cacheaux, L.P., Ivens, S., Lapilover, E., Heinemann, U., Kaufer, D., and Friedman, A. (2009). Astrocytic dysfunction in epileptogenesis: consequence of altered potassium and glutamate homeostasis? *J Neurosci* 29, 10588-10599.

Ding, F., O'Donnell, J., Thrane, A.S., Zeppenfeld, D., Kang, H., Xie, L., Wang, F., and Nedergaard, M. (2013).  $\alpha$ 1-Adrenergic receptors mediate coordinated Ca<sup>2+</sup> signaling of cortical astrocytes in awake, behaving mice. *Cell Calcium* 54, 387-394.

Dumstrei, K., Wang, F., and Hartenstein, V. (2003). Role of DE-cadherin in neuroblast proliferation, neural morphogenesis, and axon tract formation in *Drosophila* larval brain development. *J Neurosci* 23, 3325-3335.

Dunst, S., Kazimiers, T., von Zadow, F., Jambor, H., Sagner, A., Brankatschk, B., Mahmoud, A., Spann, S., Tomancak, P., Eaton, S., *et al.* (2015). Endogenously tagged rab proteins: a resource to study membrane trafficking in *Drosophila*. *Dev Cell* 33, 351-365.

Enyedi, P., and Czirjak, G. (2015). Properties, regulation, pharmacology, and functions of the K(2)p channel, TRESK. *Pflugers Arch* 467, 945-958.

Erdmann, F., Weiwad, M., Kilka, S., Karanik, M., Patzel, M., Baumgrass, R., Liebscher, J., and Fischer, G. (2010). The novel calcineurin inhibitor CN585 has potent immunosuppressive properties in stimulated human T cells. *J Biol Chem* 285, 1888-1898.

Fatatis, A., and Russell, J.T. (1992). Spontaneous changes in intracellular calcium concentration in type I astrocytes from rat cerebral cortex in primary culture. *Glia* 5, 95-104.

Fellin, T., Gomez-Gonzalo, M., Gobbo, S., Carmignoto, G., and Haydon, P.G. (2006). Astrocytic glutamate is not necessary for the generation of epileptiform neuronal activity in hippocampal slices. *J Neurosci* 26, 9312-9322.

Fellin, T., Pascual, O., Gobbo, S., Pozzan, T., Haydon, P.G., and Carmignoto, G. (2004).

Neuronal synchrony mediated by astrocytic glutamate through activation of extrasynaptic NMDA receptors. *Neuron* 43, 729-743.

Fiacco, T.A., Agulhon, C., Taves, S.R., Petravicz, J., Casper, K.B., Dong, X., Chen, J., and McCarthy, K.D. (2007). Selective stimulation of astrocyte calcium in situ does not affect neuronal excitatory synaptic activity. *Neuron* 54, 611-626.

Fiacco, T.A., and McCarthy, K.D. (2018). Multiple Lines of Evidence Indicate That Gliotransmission Does Not Occur under Physiological Conditions. *J Neurosci* 38, 3-13.

Furman, J.L., and Norris, C.M. (2014). Calcineurin and glial signaling: neuroinflammation and beyond. *J Neuroinflammation* 11, 158.

Genazzani, A.A., Carafoli, E., and Guerini, D. (1999). Calcineurin controls inositol 1,4,5-trisphosphate type 1 receptor expression in neurons. *Proc Natl Acad Sci U S A* 96, 5797-5801.

Gomez-Gonzalo, M., Losi, G., Chiavegato, A., Zonta, M., Cammarota, M., Brondi, M., Vetri, F., Uva, L., Pozzan, T., de Curtis, M., *et al.* (2010). An excitatory loop with astrocytes contributes to drive neurons to seizure threshold. *PLoS Biol* 8, e1000352.

Goto, S., Matsukado, Y., Mihara, Y., Inoue, N., and Miyamoto, E. (1986a). Calcineurin in human brain and its relation to extrapyramidal system. Immunohistochemical study on postmortem human brains. *Acta Neuropathol* 72, 150-156.

Goto, S., Matsukado, Y., Mihara, Y., Inoue, N., and Miyamoto, E. (1986b). The distribution of calcineurin in rat brain by light and electron microscopic immunohistochemistry and enzyme-immunoassay. *Brain Res* 397, 161-172.

Graef, I.A., Mermelstein, P.G., Stankunas, K., Neilson, J.R., Deisseroth, K., Tsien, R.W., and Crabtree, G.R. (1999). L-type calcium channels and GSK-3 regulate the activity of NF-ATc4 in hippocampal neurons. *Nature* 401, 703-708.

Groth, R.D., Coicou, L.G., Mermelstein, P.G., and Seybold, V.S. (2007). Neurotrophin activation of NFAT-dependent transcription contributes to the regulation of pro-nociceptive genes. *J Neurochem* 102, 1162-1174.

Haj-Yasein, N.N., Jensen, V., Vindedal, G.F., Gundersen, G.A., Klungland, A., Ottersen, O.P., Hvalby, O., and Nagelhus, E.A. (2011). Evidence that compromised K<sup>+</sup> spatial buffering contributes to the epileptogenic effect of mutations in the human Kir4.1 gene (KCNJ10). *Glia* 59, 1635-1642.

Halassa, M.M., Fellin, T., Takano, H., Dong, J.H., and Haydon, P.G. (2007). Synaptic islands defined by the territory of a single astrocyte. *J Neurosci* 27, 6473-6477.

Hwang, E.M., Kim, E., Yarishkin, O., Woo, D.H., Han, K.S., Park, N., Bae, Y., Woo, J., Kim, D., Park, M., *et al.* (2014). A disulfide-linked heterodimer of TWIK-1 and TREK-1 mediates passive conductance in astrocytes. *Nat Commun* 5, 3227.

Kataoka, A., Tozaki-Saitoh, H., Koga, Y., Tsuda, M., and Inoue, K. (2009). Activation of P2X7

receptors induces CCL3 production in microglial cells through transcription factor NFAT. *J Neurochem* 108, 115-125.

Kawasaki, F., Zou, B., Xu, X., and Ordway, R.W. (2004). Active zone localization of presynaptic calcium channels encoded by the cacophony locus of *Drosophila*. *J Neurosci* 24, 282-285.

Kuchibhotla, K.V., Lattarulo, C.R., Hyman, B.T., and Bacskai, B.J. (2009). Synchronous hyperactivity and intercellular calcium waves in astrocytes in Alzheimer mice. *Science* 323, 1211-1215.

Kuebler, D., and Tanouye, M. (2002). Anticonvulsant valproate reduces seizure-susceptibility in mutant *Drosophila*. *Brain Res* 958, 36-42.

Kuno, T., Mukai, H., Ito, A., Chang, C.D., Kishima, K., Saito, N., and Tanaka, C. (1992). Distinct cellular expression of calcineurin A alpha and A beta in rat brain. *J Neurochem* 58, 1643-1651.

Langemeyer, L., Frohlich, F., and Ungermann, C. (2018). Rab GTPase Function in Endosome and Lysosome Biogenesis. *Trends Cell Biol.*

Lee, S., Yoon, B.E., Berglund, K., Oh, S.J., Park, H., Shin, H.S., Augustine, G.J., and Lee, C.J. (2010). Channel-mediated tonic GABA release from glia. *Science* 330, 790-796.

Leis, J.A., Bekar, L.K., and Walz, W. (2005). Potassium homeostasis in the ischemic brain. *Glia* 50, 407-416.

Lin, D.T., Wu, J., Holstein, D., Upadhyay, G., Rourk, W., Muller, E., and Lechleiter, J.D. (2007). Ca<sup>2+</sup> signaling, mitochondria and sensitivity to oxidative stress in aging astrocytes. *Neurobiol Aging* 28, 99-111.

Ma, B., Xu, G., Wang, W., Enyeart, J.J., and Zhou, M. (2014). Dual patch voltage clamp study of low membrane resistance astrocytes in situ. *Mol Brain* 7, 18.

Ma, Z., Stork, T., Bergles, D.E., and Freeman, M.R. (2016). Neuromodulators signal through astrocytes to alter neural circuit activity and behaviour. *Nature* 539, 428-432.

Masuyama, K., Zhang, Y., Rao, Y., and Wang, J.W. (2012). Mapping neural circuits with activity-dependent nuclear import of a transcription factor. *J Neurogenet* 26, 89-102.

Melom, J.E., and Littleton, J.T. (2013). Mutation of a NCKX eliminates glial microdomain calcium oscillations and enhances seizure susceptibility. *J Neurosci* 33, 1169-1178.

Moia, L.J., Matsui, H., de Barros, G.A., Tomizawa, K., Miyamoto, K., Kuwata, Y., Tokuda, M., Itano, T., and Hatase, O. (1994). Immunosuppressants and calcineurin inhibitors, cyclosporin A and FK506, reversibly inhibit epileptogenesis in amygdaloid kindled rat. *Brain Res* 648, 337-341.

Moriwaki, A., Lu, Y.F., Hayashi, Y., Tomizawa, K., Tokuda, M., Itano, T., Hatase, O., and Matsui, H. (1996). Immunosuppressant FK506 prevents mossy fiber sprouting induced by kindling stimulation. *Neurosci Res* 25, 191-194.

Murphy-Royal, C., Dupuis, J., Groc, L., and Oliet, S.H.R. (2017). Astroglial glutamate transporters in the brain: Regulating neurotransmitter homeostasis and synaptic transmission. *J Neurosci Res* 95, 2140-2151.

Muthukumar, A.K., Stork, T., and Freeman, M.R. (2014). Activity-dependent regulation of astrocyte GAT levels during synaptogenesis. *Nat Neurosci* 17, 1340-1350.

Nagamoto-Combs, K., and Combs, C.K. (2010). Microglial phenotype is regulated by activity of the transcription factor, NFAT (nuclear factor of activated T cells). *J Neurosci* 30, 9641-9646.

Nakai, Y., Horiuchi, J., Tsuda, M., Takeo, S., Akahori, S., Matsuo, T., Kume, K., and Aigaki, T. (2011). Calcineurin and its regulator sra/DSCR1 are essential for sleep in *Drosophila*. *J Neurosci* 31, 12759-12766.

Nedergaard, M. (1994). Direct signaling from astrocytes to neurons in cultures of mammalian brain cells. *Science* 263, 1768-1771.

Nett, W.J., Oloff, S.H., and McCarthy, K.D. (2002). Hippocampal astrocytes in situ exhibit calcium oscillations that occur independent of neuronal activity. *J Neurophysiol* 87, 528-537.

Nimmerjahn, A., Mukamel, E.A., and Schnitzer, M.J. (2009). Motor behavior activates Bergmann glial networks. *Neuron* 62, 400-412.

Parker, L., Howlett, I.C., Rusan, Z.M., and Tanouye, M.A. (2011). Seizure and epilepsy: studies of seizure disorders in *Drosophila*. *Int Rev Neurobiol* 99, 1-21.

Parpura, V., Basarsky, T.A., Liu, F., Jęftinija, K., Jęftinija, S., and Haydon, P.G. (1994). Glutamate-mediated astrocyte-neuron signalling. *Nature* 369, 744-747.

Paukert, M., Agarwal, A., Cha, J., Doze, V.A., Kang, J.U., and Bergles, D.E. (2014). Norepinephrine controls astroglial responsiveness to local circuit activity. *Neuron* 82, 1263-1270.

Pavlidis, P., and Tanouye, M.A. (1995). Seizures and failures in the giant fiber pathway of *Drosophila* bang-sensitive paralytic mutants. *J Neurosci* 15, 5810-5819.

Pereanu, W., Shy, D., and Hartenstein, V. (2005). Morphogenesis and proliferation of the larval brain glia in *Drosophila*. *Dev Biol* 283, 191-203.

Pimentel, D., Donlea, J.M., Talbot, C.B., Song, S.M., Thurston, A.J.F., and Miesenbock, G. (2016). Operation of a homeostatic sleep switch. *Nature* 536, 333-337.

Pirttimäki, T.M., Hall, S.D., and Parri, H.R. (2011). Sustained neuronal activity generated by glial plasticity. *J Neurosci* 31, 7637-7647.

Polli, J.W., Billingsley, M.L., and Kincaid, R.L. (1991). Expression of the calmodulin-dependent protein phosphatase, calcineurin, in rat brain: developmental patterns and the role of nigrostriatal innervation. *Brain Res Dev Brain Res* 63, 105-119.

Porter, J.T., and McCarthy, K.D. (1996). Hippocampal astrocytes in situ respond to glutamate

released from synaptic terminals. *J Neurosci* 16, 5073-5081.

Reese, L.C., and Tagliatela, G. (2011). A role for calcineurin in Alzheimer's disease. *Curr Neuropharmacol* 9, 685-692.

Rieckhof, G.E., Yoshihara, M., Guan, Z., and Littleton, J.T. (2003). Presynaptic N-type calcium channels regulate synaptic growth. *J Biol Chem* 278, 41099-41108.

Rojanathammanee, L., Puig, K.L., and Combs, C.K. (2013). Pomegranate polyphenols and extract inhibit nuclear factor of activated T-cell activity and microglial activation in vitro and in a transgenic mouse model of Alzheimer disease. *J Nutr* 143, 597-605.

Rose, C.R., Felix, L., Zeug, A., Dietrich, D., Reiner, A., and Henneberger, C. (2017). Astroglial Glutamate Signaling and Uptake in the Hippocampus. *Front Mol Neurosci* 10, 451.

Rusnak, F., and Mertz, P. (2000). Calcineurin: form and function. *Physiol Rev* 80, 1483-1521.

Sama, D.M., and Norris, C.M. (2013). Calcium dysregulation and neuroinflammation: discrete and integrated mechanisms for age-related synaptic dysfunction. *Ageing Res Rev* 12, 982-995.

Savtchouk, I., and Volterra, A. (2018). Gliotransmission: Beyond Black-and-White. *J Neurosci* 38, 14-25.

Shiratori, M., Tozaki-Saitoh, H., Yoshitake, M., Tsuda, M., and Inoue, K. (2010). P2X7 receptor activation induces CXCL2 production in microglia through NFAT and PKC/MAPK pathways. *J Neurochem* 114, 810-819.

Somjen, G.G. (2002). Ion regulation in the brain: implications for pathophysiology. *Neuroscientist* 8, 254-267.

Song, J., and Tanouye, M.A. (2008). From bench to drug: human seizure modeling using *Drosophila*. *Prog Neurobiol* 84, 182-191.

Spindler, S.R., Ortiz, I., Fung, S., Takashima, S., and Hartenstein, V. (2009). *Drosophila* cortex and neuropile glia influence secondary axon tract growth, pathfinding, and fasciculation in the developing larval brain. *Dev Biol* 334, 355-368.

Srinivasan, R., Huang, B.S., Venugopal, S., Johnston, A.D., Chai, H., Zeng, H., Golshani, P., and Khakh, B.S. (2015). Ca(2+) signaling in astrocytes from *Ip3r2(-/-)* mice in brain slices and during startle responses in vivo. *Nat Neurosci* 18, 708-717.

Stork, T., Sheehan, A., Tasdemir-Yilmaz, O.E., and Freeman, M.R. (2014). Neuron-glia interactions through the Heartless FGF receptor signaling pathway mediate morphogenesis of *Drosophila* astrocytes. *Neuron* 83, 388-403.

Takasaki, C., Yamasaki, M., Uchigashima, M., Konno, K., Yanagawa, Y., and Watanabe, M. (2010). Cytochemical and cytological properties of perineuronal oligodendrocytes in the mouse cortex. *Eur J Neurosci* 32, 1326-1336.



Takata, N., and Hirase, H. (2008). Cortical layer 1 and layer 2/3 astrocytes exhibit distinct calcium dynamics in vivo. *PLoS One* 3, e2525.

Takeo, S., Tsuda, M., Akahori, S., Matsuo, T., and Aigaki, T. (2006). The calcineurin regulator sra plays an essential role in female meiosis in *Drosophila*. *Curr Biol* 16, 1435-1440.

Tasdemir-Yilmaz, O.E., and Freeman, M.R. (2014). Astrocytes engage unique molecular programs to engulf pruned neuronal debris from distinct subsets of neurons. *Genes Dev* 28, 20-33.

Tashiro, A., Goldberg, J., and Yuste, R. (2002). Calcium oscillations in neocortical astrocytes under epileptiform conditions. *J Neurobiol* 50, 45-55.

Tian, G.F., Azmi, H., Takano, T., Xu, Q., Peng, W., Lin, J., Oberheim, N., Lou, N., Wang, X., Zielke, H.R., *et al.* (2005). An astrocytic basis of epilepsy. *Nat Med* 11, 973-981.

Tomita, J., Mitsuyoshi, M., Ueno, T., Aso, Y., Tanimoto, H., Nakai, Y., Aigaki, T., Kume, S., and Kume, K. (2011). Pan-neuronal knockdown of calcineurin reduces sleep in the fruit fly, *Drosophila melanogaster*. *J Neurosci* 31, 13137-13146.

Ventura, R., and Harris, K.M. (1999). Three-dimensional relationships between hippocampal synapses and astrocytes. *J Neurosci* 19, 6897-6906.

Verstreken, P., Kjaerulff, O., Lloyd, T.E., Atkinson, R., Zhou, Y., Meinertzhagen, I.A., and Bellen, H.J. (2002). Endophilin mutations block clathrin-mediated endocytosis but not neurotransmitter release. *Cell* 109, 101-112.

Volkenhoff, A., Weiler, A., Letzel, M., Stehling, M., Klambt, C., and Schirmeier, S. (2015). Glial Glycolysis Is Essential for Neuronal Survival in *Drosophila*. *Cell Metab* 22, 437-447.

Wang, F., Smith, N.A., Xu, Q., Fujita, T., Baba, A., Matsuda, T., Takano, T., Bekar, L., and Nedergaard, M. (2012a). Astrocytes modulate neural network activity by Ca<sup>2+</sup>-dependent uptake of extracellular K<sup>+</sup>. *Sci Signal* 5, ra26.

Wang, F., Xu, Q., Wang, W., Takano, T., and Nedergaard, M. (2012b). Bergmann glia modulate cerebellar Purkinje cell bistability via Ca<sup>2+</sup>-dependent K<sup>+</sup> uptake. *Proc Natl Acad Sci U S A* 109, 7911-7916.

Wang, W., Kiyoshi, C.M., Du, Y., Ma, B., Alford, C.C., Chen, H., and Zhou, M. (2016). mGluR3 Activation Recruits Cytoplasmic TWIK-1 Channels to Membrane that Enhances Ammonium Uptake in Hippocampal Astrocytes. *Mol Neurobiol* 53, 6169-6182.

Wang, X., Lou, N., Xu, Q., Tian, G.F., Peng, W.G., Han, X., Kang, J., Takano, T., and Nedergaard, M. (2006). Astrocytic Ca<sup>2+</sup> signaling evoked by sensory stimulation in vivo. *Nat Neurosci* 9, 816-823.

Wetherington, J., Serrano, G., and Dingledine, R. (2008). Astrocytes in the epileptic brain. *Neuron* 58, 168-178.

White, B.H., Osterwalder, T.P., Yoon, K.S., Joiner, W.J., Whim, M.D., Kaczmarek, L.K., and Keshishian, H. (2001). Targeted attenuation of electrical activity in *Drosophila* using a genetically modified K(+) channel. *Neuron* 31, 699-711.

Woo, D.H., Han, K.S., Shim, J.W., Yoon, B.E., Kim, E., Bae, J.Y., Oh, S.J., Hwang, E.M., Marmorstein, A.D., Bae, Y.C., *et al.* (2012). TREK-1 and Best1 channels mediate fast and slow glutamate release in astrocytes upon GPCR activation. *Cell* 151, 25-40.

Xie, Z., Long, J., Liu, J., Chai, Z., Kang, X., and Wang, C. (2017). Molecular Mechanisms for the Coupling of Endocytosis to Exocytosis in Neurons. *Front Mol Neurosci* 10, 47.

Zhang, Y.V., Ormerod, K.G., and Littleton, J.T. (2017). Astrocyte Ca(2+) Influx Negatively Regulates Neuronal Activity. *eNeuro* 4.

Zhou, Y., Cameron, S., Chang, W.T., and Rao, Y. (2012). Control of directional change after mechanical stimulation in *Drosophila*. *Mol Brain* 5, 39.